THE JOURNAL OF BIOLOGICAL CHEMISTRY VOL. 287, NO. 20, pp. 16132–16145, May 11, 2012
Published in the U.S.A.

TRAF6 Protein Couples Toll-like Receptor 4 Signaling to Src Family Kinase Activation and Opening of Paracellular Pathway in Human Lung Microvascular Endothelia*

Received for publication, October 4, 2011, and in revised form, March 2, 2012 Published, JBC Papers in Press, March 23, 2012, DOI 10.1074/jbc.M111.310102

Anguo Liu[‡§1], Ping Gong[‡§1], Sang W. Hyun[‡§], Kent Z. Q. Wang[¶], Elizabeth A. Cates[‖], Darren Perkins[**], Douglas D. Bannerman[‡§], Adam C. Puché[‡‡], Vladimir Y. Toshchakov[**], Shengyun Fang[§§¶¶], Philip E. Auron[¶], Stefanie N. Vogel[‡], and Simeon E. Goldblum[‡§‖‖2]**

From the [‡]Mucosal Biology Research Center, Departments of [§]Medicine, [**]Microbiology and Immunology, and [‡‡]Anatomy and Neurobiology and [§§]Center for Biomedical Engineering and Technology, [¶¶]Department of Physiology, University of Maryland, Baltimore, Maryland 21201, the [‖‖]Veterans Affairs Maryland Health Care System, Baltimore, Maryland 21201, the [¶]Department of Biological Sciences, Duquesne University, Pittsburgh, Pennsylvania 15282, and the [‖]Department of Cell Biology and Molecular Genetics, University of Maryland, College Park, Maryland 20742-6105

Background: Bacterial lipopolysaccharide (LPS) disrupts endothelial barrier integrity.
Results: LPS increases association of a TRAF6 proline-rich SH3-binding motif (aa 461–469) with c-Src and Fyn, followed by their ubiquitination and activation, which in turn increases endothelial paracellular permeability.
Conclusion: TRAF6 couples LPS stimulation to Src family kinase activation and loss of endothelial barrier integrity.
Significance: TRAF6 offers a target for therapeutic intervention for LPS-induced pulmonary microvascular endothelial injury.

Gram-negative bacteria release lipopolysaccharide (LPS) into the bloodstream. Here, it engages Toll-like receptor (TLR) 4 expressed in human lung microvascular endothelia (HMVEC-Ls) to open the paracellular pathway through Src family kinase (SFK) activation. The signaling molecules that couple TLR4 to the SFK-driven barrier disruption are unknown. In HMVEC-Ls, siRNA-induced silencing of TIRAP/Mal and overexpression of dominant-negative TIRAP/Mal each blocked LPS-induced SFK activation and increases in transendothelial [^{14}C]albumin flux, implicating the MyD88-dependent pathway. LPS increased TRAF6 autoubiquitination and binding to IRAK1. Silencing of TRAF6, TRAF6-dominant-negative overexpression, or preincubation of HMVEC-Ls with a cell-permeable TRAF6 decoy peptide decreased both LPS-induced SFK activation and barrier disruption. LPS increased binding of both c-Src and Fyn to GST-TRAF6 but not to a GST-TRAF6 mutant in which the three prolines in the putative Src homology 3 domain-binding motif (amino acids 461–469) were substituted with alanines. A cell-permeable decoy peptide corresponding to the same proline-rich motif reduced SFK binding to WT GST-TRAF6 compared with the Pro → Ala-substituted peptide. Finally, LPS increased binding of activated Tyr(P)^{416}-SFK to GST-TRAF6, and preincubation of HMVEC-Ls with SFK-selective tyrosine kinase inhibitors, PP2 and SU6656, diminished TRAF6 binding to c-Src and Fyn. During the TRAF6-SFK association, TRAF6 catalyzed Lys^{63}-linked ubiquitination of c-Src and Fyn, whereas SFK activation increased tyrosine phosphorylation of TRAF6. The TRAF6 decoy peptide blocked both LPS-induced SFK ubiquitination and TRAF6 phosphorylation. Together, these data indicate that the proline-rich Src homology 3 domain-binding motif in TRAF6 interacts directly with activated SFKs to couple LPS engagement of TLR4 to SFK activation and loss of barrier integrity in HMVEC-Ls.

Gram-negative sepsis and its attendant endotoxemia can be complicated by life-threatening vascular leak syndromes, including the acute respiratory distress syndrome (1). The Gram-negative bacterial component responsible for this loss of endothelial barrier integrity is the outer membrane constituent, endotoxin or lipopolysaccharide (LPS) (2, 3). We have previously established that LPS directly opens the endothelial paracellular pathway (2, 3) and requires LPS-binding protein (4), soluble CD14 (4), and Toll-like receptor 4 (TLR4)[3] expression (5) for optimal presentation to the endothelial cell (EC) surface. In human lung microvascular EC (HMVEC-L), LPS activates Src family kinase (SFK) and increases tyrosine phosphorylation of components within the EC-EC adherens junction or zonula adherens multiprotein complex, coincident with barrier disruption (5). Prior broad spectrum SFK inhibition protected against both zonula adherens protein tyrosine phosphorylation and barrier disruption (5). In these same studies, we found that four members of the SFK family, c-Src, Fyn, Yes, and Lyn, were expressed in HMVEC-Ls and that selective silencing of c-Src,

* This work was supported, in whole or in part, by National Institutes of Health Grants HL089179 (to S. E. G.), AI18797 (to S. N. V.), and AI082299 (to V. Y. T.). This work was also supported by a Merit Review grant from the Department of Veterans Affairs (to S. E. G.).

[1] Both authors contributed equally to this work.

[2] To whom correspondence should be addressed: Mucosal Biology Research Center, University of Maryland School of Medicine, 20 Penn St., Rm. 351, Baltimore, MD 21201. Tel.: 410-706-5504; Fax: 410-706-5508; E-mail: sgoldblu@mbrc.umaryland.edu.

[3] The abbreviations used are: TLR4, Toll-like receptor 4; EC, endothelial cell; Ad, adenovirus; DN, dominant-negative; HMVEC-L, human lung microvascular EC; MATH domain, Meprin and TRAF homology domain; m.o.i., multiplicity of infection; RING, really interesting new gene; SFK, Src family kinase; SH domain, Src homology; SP, scrambled peptide; TIR domain, Toll/IL-1 receptor resistance homology domain; TIRAP, TIR domain-containing adapter protein; aa, amino acid.

Fyn, and Yes, but not Lyn, each diminished both LPS-induced tyrosine phosphorylation of vascular endothelial-cadherin and p120 catenin and barrier disruption (5).

The structure of SFKs is highly conserved (6, 7). Each contains an NH_2-terminal myristoylated region, a 50–70-amino acid region unique to each family member, an Src homology (SH)3 domain, an SH2 domain, a short linker region, a catalytic domain, and the regulatory COOH terminus. Upon activation, the inactive enzyme, which resides in a perinuclear location, is translocated to the cell periphery where the myristoylated NH_2 terminus facilitates attachment to the plasma membrane. The SH3 domain recognizes proline-rich sequences, whereas the SH2 domain recognizes phosphotyrosine-containing proteins. The kinase domain contains a Tyr^{416} within its activation loop that is autophosphorylated upon activation. The COOH terminus contains a Tyr^{527} that is phosphorylated in the restrained state. Low affinity intramolecular associations between the SH2 domain and phosphorylated Tyr^{527} and between SH3 and the short linker region maintain the SFK in an autoinhibited conformation. High affinity binding partners for the SH2 and/or SH3 domains that competitively disrupt these autoinhibitory intramolecular interactions activate SFK activity (8).

TLR4 is the principal signal-transducing receptor for LPS (9, 10). TLR4 is a membrane-spanning protein composed of an NH_2-terminal ectodomain with leucine-rich repeats that binds an extracellular protein, MD2, that is required for ligand recognition, a transmembrane region, and an intracellular region that includes a conserved Toll/IL-1 receptor resistance (TIR) homology domain that participates in protein-protein interactions and downstream signaling (11, 12). TIR domain-containing adapter protein (TIRAP), also called MyD88 adapter-like (Mal), constitutively associates with the TIR motif of TLR4 (11, 13). TIRAP/Mal contains a phosphatidylinositol 4,5-bisphosphate-binding domain that mediates its recruitment to the plasma membrane (14). Upon LPS interaction with MD2, TLR4 dimerizes (12). Myeloid differentiation factor 88 (MyD88), another TIR domain-containing adapter molecule that also contains an NH_2-terminal death domain, is recruited to and associates with TLR4 and TIRAP/Mal through TIR domain interactions (13, 15). TIRAP-facilitated recruitment of MyD88 to the TLR4 receptor complex initiates the MyD88-dependent signaling pathway that has been implicated in LPS-induced tyrosine phosphorylation events (16, 17). MyD88 recruits the serine/threonine kinases, IL-1 receptor-associated kinase (IRAK) 1 and 4 (18). IRAK4 phosphorylates IRAK1 that undergoes a conformational change and autophosphorylation, after which IRAK1 dissociates from the TLR4 complex and forms a complex with tumor necrosis factor (TNF) α-associated factor (TRAF) 6 in the cytoplasm (18). More recently, IRAK2 has been reported to play a more active role than IRAK1 in TLR4-mediated TRAF6 activation (19–21). TRAF6 forms a complex with transforming growth factor-β-activated kinase (TAK1), TAK1-binding protein (TAB) 1 and TAB2, which through activation of multiple transcription factors up-regulates proinflammatory gene expression (22, 23). Although it is well known that LPS elicits a wide range of host cell responses, studies of downstream TLR4 signaling have largely focused on signaling events that promote such gene expression. Furthermore, much of our understanding of TLR4 signaling has been established in cells of monocyte/macrophage lineage where both TLR4 and CD14 are highly expressed on the cell surface (24). In ECs, a major target for circulating intravascular LPS, far less is understood (25, 26). Hence, the one or more signaling molecules that couple the TLR4-LPS interaction in ECs to SFK activation and barrier disruption are not known.

A candidate molecule that might extend the TLR4 signaling pathway to SFK activation is the cytoplasmic adapter protein TRAF6. In multiple non-EC systems, including osteoclasts, monocytes, dendritic cells, and glioblastoma and embryonic cell lines, TRAF6 interacts with c-Src after ligation of the type 1 interleukin (IL)-1 receptor (27–29) and members of the TNF receptor superfamily, including CD40 (30) and TNF-related activation-induced cytokine-R (31). Furthermore, $TRAF6^{-/-}$ and $c\text{-}Src^{-/-}$ mice share an unusual phenotype, osteopetrosis (32, 33). All six members of the TRAF family contain a TRAF domain composed of a coiled-coil region in tandem with a more highly conserved COOH-terminal immunoglobulin-like Meprin and TRAF Homology (MATH) domain (27, 30, 34). The MATH domain participates in recruitment of TRAF proteins to receptors, multimerization with other TRAF molecules, and binding to IRAKs (27, 30, 34, 35). TRAF2–6 each contain an NH_2-terminal RING finger domain with multiple zinc finger-like motifs (27, 30, 34). The RING domain, in concert with the first zinc finger region, permits TRAF6 to function as an autocatalytic Lys^{63} ubiquitin ligase required for downstream MAPK and NF-κB activation (27, 34, 36, 37). Of relevance to this study, TRAF6 contains within its MATH domain a proline-rich, putative SH3-binding motif, RPTIPRNPK (aa 461–469), which is required for its physical association with c-Src (27, 31). However, this same TRAF6 sequence is insufficient for SFK activation (31), suggesting that additional sequences in TRAF6 regulate SFK catalytic activity. In this study, we define the molecular interaction through which TRAF6 couples LPS engagement of TLR4 to SFK activation and loss of barrier integrity in HMVEC-Ls. More specifically, TRAF6 physically interacts with SFKs, and during this interaction, TRAF6 catalyzes Lys^{63}-linked ubiquitination of SFKs that in turn reciprocally tyrosine phosphorylate TRAF6 in response to LPS.

EXPERIMENTAL PROCEDURES

Reagents—Protein-free *Escherichia coli* K235 LPS (<0.008% protein) was prepared by a double hot phenol/water extraction method to exclude contaminating bacterial constituents (5). The SFK inhibitors, PP2 and SU6656, were purchased from Calbiochem. [^{14}C]Bovine serum albumin (BSA) was purchased from Sigma.

HMVEC-L Culture—HMVEC-Ls (Lonza, Rockland, ME) were cultured in EC growth medium (EBM-2; Lonza) containing 5% fetal bovine serum, human recombinant epidermal growth factor, human recombinant insulin-like growth factor-1, human basic fibroblast growth factor, vascular endothelial growth factor, hydrocortisone, ascorbic acid, gentamicin, and amphotericin B (5). HMVEC-Ls at passages 5–10 were studied. Trypan blue exclusion was used to assess EC viability.

Construction of Adenovirus Encoding for DN TIRAP and Wild Type (WT) and DN TRAF6—To generate the TIRAP DN construct, primers were designed to amplify the entire coding region of bovine TIRAP (NM_001039962), which is highly homologous with human TIRAP (38). The forward primer (5′-CCGGAATTCATGGCATCATCAACCTCC-3′) and the reverse primer (5′-CCGCTCGAGCTATCAGCCAAGGGTC-TGCAG-3′) were utilized for PCR amplification, after which Pro^{136} in the construct was mutated to His^{136} using the QuikChange site-directed mutagenesis kit (Stratagene, Inc., La Jolla, CA) using the following primers: 5′-CTTCGCGACGCC-ACCCATGGTGGCGCCATCGTG-3′) and 5′-CACGATGG-CGCCACCATGGGTGGCGTCGCGAAG-3′. In other experiments, primers were designed to amplify sequence encoding amino acids 307–542 of bovine TRAF6 (NM_001034661/NP_001029833), which is highly homologous with the corresponding region of human TRAF6 (38). The forward primer (5′-CCGGAATTCGGGCGTCACTCAGAAGTCCAC-3′) and the reverse primer (5′-CCGCTCGAGCTACTATATCCCTGAGT-CAGTACT-3′) were used for PCR amplification. In each case, the primers also included sequences encoding 5′ EcoRI and 3′ XhoI restriction sites to enable subsequent insertion of the construct into the pCR3.V64 Met FLAG vector (gift from Dr. Jurg Tschopp, Institute of Biochemistry of the University of Lausanne, Switzerland). PCR amplification was performed using first strand cDNA, which was generated from bovine mammary epithelial cell RNA, iQ Supermix (Bio-Rad), and the primers described above. The cycling conditions were 95 °C for 3 min, followed by 35 cycles of the following: 95 °C for 30 s, 55 °C for 30 s, and 72 °C for 1 min. The PCR products were digested with EcoRI and XhoI and ligated into the pCR3.V64 Met FLAG vector. This vector contains a 5′ BamHI site followed by a coding region for an initiator methionine, a FLAG tag (DYKDDDDK), and a spacer of two amino acids (EF) immediately before the EcoRI-XhoI PCR product insertion site. Bacteria were transformed with the ligation reactions, and clones from bacteria containing appropriately sized inserts were fully sequenced. The entire expression cassette, encoding the FLAG tag and either the TIRAP DN or TRAF6 DN construct, was transferred into an adenovirus (Ad) genome vector (adenovirus type 5 (dE1/E3)), and virus expressing the construct was generated by Vector Biolabs (Philadelphia, PA). Ad constructs encoding for WT c-Src and Fyn were purchased from Vector Biolabs.

Ad Infection to Overexpress DN TIRAP, WT and DN TRAF6, and WT c-Src and Fyn—Each Ad construct was linearized with PacI digestion and transfected, in the presence of Ca_2PO_4, into HEK293T cells. After 7–10 days, cells were scraped off flasks with a rubber policeman and subjected to three freeze-thaw cycles, and virus was harvested in the supernatants for infection of fresh HEK293 T cells and titration in a plaque-forming assay. HMVEC-Ls were transiently infected with packaged Ad at an increasing m.o.i. or an Ad-null vector control. At 48 h, cells were lysed, and the lysates processed for FLAG, c-Src, or Fyn immunoblotting. To control for protein loading and transfer, blots were stripped and reprobed for β-tubulin. These Ad-infected HMVEC-Ls were used for assays to detect SFK activation, binding to glutathione *S*-transferase (GST)-TRAF6, and barrier dysfunction.

Detection of SFK Activity by Cell-based ELISA and Phospho-SFK Immunoblotting—HMVEC-Ls (1.5×10^4 cells/well) were cultured for 48 h in flat bottom 96-well plates, after which they were exposed for increasing times to increasing concentrations of LPS or medium alone, as described previously (5). The cells were fixed, washed, quenched with H_2O_2 and NaN_3, and microwaved, according to the manufacturer's protocol (SuperArray). The plates were washed, blocked, incubated with anti-phospho-SFK (Tyr^{416}) or anti-pan-SFK antibodies, washed, and incubated with secondary antibody. The plates were incubated with developing solution, and the $A_{450\ nm}$ for each well was determined, as described previously (5). To normalize each well to relative cell number, the plates were washed, dried, incubated with protein stain, again washed, and solubilized in 1% SDS, and the $A_{595\ nm}$ was determined. Each phospho-SFK and each pan-SFK well was normalized to cell number in the same well, and each normalized phospho-SFK value was expressed relative to its normalized pan-SFK value. SFK activity was calculated as phospho-SFK A_{450}/A_{595} per pan-SFK A_{450}/A_{595}.

In other experiments, HMVEC-Ls were lysed, and the lysates were processed for immunoblotting with rabbit polyclonal anti-human phospho-SFK (Tyr^{416}) antibody (Cell Signaling Technology, Danvers, MA) followed by horseradish peroxidase (HRP)-conjugated goat anti-rabbit IgG (Cell Signaling Technology). To confirm equivalent protein loading and transfer, blots were stripped with 100 mM 2-mercaptoethanol, 2% SDS, 62.5 mmol/liter Tris-HCl, pH 6.7, and reprobed with murine monoclonal anti-β-tubulin (Invitrogen) followed by HRP-conjugated goat anti-mouse IgG (Invitrogen). Blots were developed by enhanced chemiluminescence (ECL). Densitometric quantification of phospho-SFK signal in each lane was normalized to total SFK signal in the same lane.

Expression of TRAF6 Protein in HMVEC-Ls—To assess TRAF6 expression at the protein level, HMVEC-Ls were thoroughly rinsed with ice-cold HEPES buffer and solubilized with ice-cold lysis buffer as described previously (5). The cell lysates were assayed for protein concentration with a DC protein assay kit (Bio-Rad). Equal amounts of protein were resolved by SDS-PAGE (8–16% gel; Novex, San Diego) and transferred to polyvinylidene fluoride (PVDF) membranes (Millipore, Bedford, MA). The blots were blocked for 1 h using 5% nonfat milk in TBS/Tween buffer and probed with rabbit polyclonal anti-TRAF6 IgG (Santa Cruz Biotechnology) followed by HRP-conjugated goat anti-rabbit antibodies (Cell Signaling; Danvers, MA) in 5% milk, TBS-T and developed with ECL. To control for protein loading and transfer, blots were stripped and reprobed with 0.5 ng/ml murine anti-physarum β-tubulin IgG2b (Roche Applied Science) followed by HRP-conjugated anti-mouse IgG (Transduction Laboratories) and again developed with ECL.

Detection of TRAF6 and SFK Ubiquitination—HMVEC-Ls were incubated for 15 min with LPS (300 ng/ml) or medium alone and solubilized in lysis buffer, and the lysates were immunoprecipitated with either rabbit anti-human TRAF6, c-Src, or Fyn IgG (all from Santa Cruz Biotechnology) or murine monoclonal anti-ubiquitin (Clone PD4) antibody (Cell Signaling), as described previously (5). Each immunoprecipitate was resolved by SDS-PAGE and transferred to PVDF membrane. The blots of the TRAF6, c-Src, and Fyn immunoprecipitates were probed

TABLE 1
TRAF6 decoy and control peptides
Each peptide was synthesized in tandem with the cell-permeating 16-amino acid sequence of the *D. antennapedia* homeodomain.

Peptide	Sequence
TRAF6 proline-rich SH3-binding motif peptide[a]	RQIKIWGQNRRMKWKKAQRPTIPRNPKGA
Mutated TRAF6 P3A control peptide[b]	RQIKIWFQNRRMKWKKAQRATIARNAKGA
Scrambled amino acid control peptide (SP)[c]	RQIKIWFQNRRMKWKKSLHGRGDPMEAFII

[a] This is based on the proline-rich putative SH3-binding motif (RPTIPRNPK, amino acids 461–469) in TRAF6 (18, 25).
[b] Control peptide in which the three underlined prolines each have been substituted with an alanine is shown.
[c] Control peptide with scrambled amino acid sequence is shown.

with anti-ubiquitin antibody followed by HRP-conjugated anti-mouse IgG (Thermo), whereas the blots of the polyubiquitinated immunoprecipitates were probed with antibodies raised against TRAF6, Src, or Fyn followed by HRP-conjugated goat anti-rabbit antibodies (Cell Signaling). In other experiments, lysates of LPS-treated and medium control HMVEC-Ls were immunoprecipitated with rabbit monoclonal anti-ubiquitin (Lys^{63}-specific) antibody (Millipore Corp., Billerica, MA). In selected experiments, these same lysates were immunoprecipitated with antibodies raised against TRAF6, Fyn, and c-Src. Here, the immune complexes immobilized on agarose beads were resuspended in 2% SDS and heat-treated (90% for 5 min) to disassemble the multiprotein complexes, as described previously (39). The protein mixture suspended in the SDS-containing buffer was diluted in PBS to reconstitute antibody function and re-immunoprecipitated with the same anti-TRAF6, anti-Fyn, and anti-c-Src antibodies. The TRAF6, Fyn, and c-Src immunoprecipitates were processed for Lys^{63}-specific ubiquitin immunoblotting. All blots were developed with ECL. To control for efficiency of immunoprecipitation and protein loading and transfer, the blots were stripped and reprobed with the immunoprecipitating antibodies.

Knockdown of TIRAP and TRAF6 through siRNA Technology—HMVEC-Ls were transfected with small interfering RNA (siRNA) duplex products designed to target either TIRAP or TRAF6 or an irrelevant control siRNA duplex that does not correspond to any known sequence in the human genome (Dharmacon, Lafayette, CO), as described previously (5, 40). For transfection, 5×10^5 HMVEC-Ls were centrifuged ($200 \times g$, 10 min), and the HMVEC-L pellet resuspended in 100 μl of Nucleofactor solution (Amaxa Biosystems) with 2.7 μg of siRNA duplexes was subjected to programmed electroporation (Program S-005, Amaxa Biosystems). The transfected cells were cultured for 24–72 h after which they were lysed, and the lysates were processed for either TIRAP (murine monoclonal anti-TIRAP IgG; Santa Cruz Biotechnology) or TRAF6 (rabbit polyclonal anti-TRAF6 IgG; Santa Cruz Biotechnology) immunoblotting. To control for protein loading and transfer, blots were stripped and reprobed for β-tubulin.

Construction of Glutathione S-Transferase (GST)-TRAF6 Wild Type and Mutant Fusion Proteins—WT TRAF6 contains a proline-rich putative SH3-binding motif (aa 461–469) (27, 31). A TRAF6 mutant was constructed in which the three prolines within the proline-rich SH3-binding motif were substituted with alanines (TRAF6 P3A) (27). WT GST-TRAF6 (aa 1–507) and the GST-TRAF6 P3A mutant were constructed as follows. TRAF6 (aa 1–507) and TRAF6 P3A fragments were isolated from TRAF6(1–507)-YEP pFLAG-CMV-5a and TRAF6 P3A YEP pFLAG-CMV-5a, respectively (27), through enzyme EcoRI/EcoRV digestion and were inserted into pGEX 5X-3 (Amersham Biosciences) treated with SalI, Klenow fragment, and EcoRI. The resulting WT GST-TRAF6 (aa 1–507) and GST-TRAF6 P3A were each introduced into BL21 strain, and their expression was verified by isopropyl 1-thio-β-D-galactoside induction (100 μM, 4 h at 37 °C) as described for other GST fusion proteins (41).

Glutathione S-Transferase (GST)-TRAF6 Binding Assays—HMVEC-Ls were transiently infected with Ad-c-Src or Ad-Fyn (m.o.i. = 200) and cultured to confluence in the wells of 100-mm dishes. The HMVEC-L monolayers were exposed for increasing times to increasing concentrations of LPS or medium alone after which the cells were lysed. In selected experiments, the cells were preincubated with PP2 (5 μM), SU6656 (10 μM), or medium alone as described previously (5). The lysates were incubated for 3 h at 4 °C with GST fusion proteins of WT TRAF6 or the TRAF6 P3A mutant coupled to glutathione-Sepharose 4B beads (Pharmacia, Piscataway, NJ), as described previously (41). The TRAF6-binding proteins bound to the beads were extensively washed, boiled in sample buffer, resolved by SDS-PAGE, and transferred to PVDF membrane. The TRAF6-binding proteins were probed with rabbit polyclonal antibodies raised against human IRAK1 (Cell Signaling Technology), c-Src (Santa Cruz Biotechnology), Fyn (Santa Cruz Biotechnology), or phospho-SFK (Tyr^{416}) (Cell Signaling Technology), each followed by HRP-conjugated goat anti-rabbit antibodies (Cell Signaling Technology). Simultaneous GST bead controls were performed.

TRAF6 Decoy Peptides—Cell-permeable decoy peptides based on the proline-rich putative SH3-binding motif (RPTIPRNPK, aa 461–469, Gene ID 22034) in TRAF6 were synthesized in tandem with the cell-permeating 16-aa sequence of the *Drosophila antennapedia* homeodomain (Table 1), as described previously (42, 43). A control peptide in which the three prolines were each substituted with an alanine was synthesized (Table 1) as was a scrambled peptide (SP) shown by Basic Local Alignment Search Tool (BLAST) not to be homologous to known proteins (Table 1) (42). Each peptide sequence is presented in Table 1. Peptides were synthesized and purified by HPLC in the Biopolymer and Genomics Core Facility (University of Maryland, Baltimore). Purity was confirmed by mass spectrometry. Stocks were dissolved in 25% DMSO and frozen at −80 °C. These peptides were studied in the following: 1) an assay for SFK activity; 2) GST-TRAF6 binding assays; 3) SFK Lys^{63}-linked ubiquitination; 4) TRAF6 phosphotyrosine immunoblotting, and 5) barrier assays.

Detection of TRAF6 Tyrosine Phosphorylation—HMVEC-Ls were preincubated for 0.5 h with PP2 (5 μM), SU6656 (5 μM), or medium alone, after which they were treated for 0.5 h with LPS (300 ng/ml) or medium alone and lysed, and the lysates were immunoprecipitated with rabbit anti-human TRAF6 antibodies. In selected experiments, the immune complexes were resuspended in 2% SDS to disrupt the multiprotein complexes, diluted, and then re-immunoprecipitated with anti-TRAF6 antibodies as described previously (39). The TRAF6 immunoprecipitates were resolved by SDS-PAGE, transferred to PVDF, and the blots probed with Tyr(P)-plus murine anti-phosphotyrosine antibody (Invitrogen) as described previously (5). To control for efficiency of immunoprecipitation and protein loading and transfer, the blots were stripped and probed with the immunoprecipitating anti-TRAF6 antibodies.

Assay of Transendothelial Albumin Flux—Transendothelial [^{14}C]BSA flux was assayed as described previously (4, 5). Briefly, gelatin-impregnated polycarbonate filters mounted in chemotactic chambers were inserted into wells of 24-well plates. HMVEC-Ls (2×10^5 cells/chamber) transfected with TRAF6-targeting or control siRNAs, or infected with Ad-TIRAP-DN, Ad-TRAF6-DN, or the Ad-Null control, or preincubated with the TRAF6 decoy or control peptides were cultured to postconfluence in each upper compartment. After the base-line transendothelial [^{14}C]BSA flux across each monolayer was established, only those monolayers retaining ≥97% of the tracers were studied. The monolayers were then exposed to LPS (100 ng/ml) or medium alone after which transendothelial [^{14}C]BSA flux was again assayed.

Statistics—One-way analysis of variance with repeated measures, followed by post hoc comparisons using Tukey's multiple paired comparison test, was used to compare the mean responses among experimental and control groups for all experiments. The GraphPad PRISM 4 program was used for these analyses. A p value of <0.05 was considered significant.

RESULTS

LPS/TLR4 Activates SFK and Disrupts Barrier Integrity through the MyD88-dependent Pathway—LPS engagement of TLR4 activates both MyD88-dependent and MyD88-independent signaling pathways (12, 15, 18). We first asked whether TLR4-mediated SFK activation and barrier disruption in HMVEC-Ls were MyD88-dependent. In response to LPS, MyD88 is recruited to the TLR4 signaling complex through a "bridging" adapter, TIRAP/Mal, through homotypic TIR domain interactions (15). To establish whether TIRAP/Mal is necessary for LPS-induced SFK activation in HMVEC-Ls, two TIRAP targeting interventions were utilized as follows: 1) siRNA-induced silencing of TIRAP/Mal and 2) overexpression of TIRAP-DN. Prior transfection of TIRAP targeting siRNAs reduced TIRAP protein ≥95% relative to that seen in control siRNA-transfected cells (Fig. 1*A*). Prior knockdown of TIRAP diminished LPS-induced SFK activation by >80% compared with the control siRNA-transfected cells (Fig. 1, *B*, *lane 4 versus 3*; and *C*). Transient infection of HMVEC-Ls with increasing m.o.i. of Ad-TIRAP-DN resulted in dose-dependent overexpression of the FLAG-tagged TIRAP-DN (Fig. 1*D*). Prior infection of HMVEC-Ls with Ad-TIRAP DN (m.o.i. = 30) blocked LPS-induced SFK activation by 90% compared with the Ad-null infected controls (Fig. 1, *E*, *lane 6 versus 4* and *2*; and *F*). Infection of HMVEC-Ls with increasing m.o.i. of Ad-TIRAP DN also dose-dependently protected against barrier disruption (Fig. 1*G*). At an m.o.i. = 30, infection with Ad-TIRAP-DN protected against >90% of barrier disruption compared with the Ad-null infected controls. These data indicate that SFK activation and barrier disruption in response to the LPS stimulus requires TIRAP/Mal for initiation of the MyD88-dependent pathway.

LPS-induced TRAF6 Activation—Upon activation, TRAF6 associates with IRAK1 (18), and as an autocatalytic ubiquitin ligase, TRAF6 becomes polyubiquitinated (36, 37). To establish that TRAF6 could be activated in HMVEC-Ls in response to LPS, these two events, *i.e.* its association with IRAK1 and its ubiquitination, were studied (Fig. 2). When lysates of LPS-treated and medium control HMVEC-Ls were incubated with WT GST-TRAF6 coupled to glutathione-Sepharose beads, LPS transiently increased IRAK1 binding to TRAF6 at 3 min (*lane 2*) and 15 min (*lane 3*), compared with the medium control (*lane 1*), with a return to base line by 30 min (*lane 4*, Fig. 2*A*). This increase in the association of IRAK1 with TRAF6 paralleled increases previously reported for SFK activation in the identical experimental system (5). Lysates of LPS-treated and medium control HMVEC-Ls were reciprocally immunoprecipitated with anti-TRAF6 and anti-ubiquitin antibodies. The TRAF6 immunoprecipitates were processed for ubiquitin immunoblotting, and the polyubiquitinated immunoprecipitates were processed for TRAF6 immunoblotting. In these experiments, LPS increased TRAF6 ubiquitination (*lanes 2* and *4*) compared with the simultaneous medium controls (*lanes 1* and *3*, Fig. 2*B*). These combined results indicate that TRAF6 is activated in HMVEC-Ls in response to LPS, and its activation temporally coincides with SFK activation (5).

TRAF6 Essential to LPS-induced SFK Activation—In non-EC systems, TRAF6 has been reported to associate with and activate c-Src (27–31). To establish whether TRAF6 is necessary for LPS-induced SFK activation in HMVEC-Ls, three TRAF6-targeting interventions were utilized as follows: 1) siRNA-induced silencing of TRAF6; 2) overexpression of TRAF6-DN, and 3) cell-permeable decoy peptides corresponding to the proline-rich putative SH3-binding motif in the MATH domain of TRAF6. Prior transfection of TRAF6-targeting siRNAs reduced TRAF6 protein (Fig. 3*A*) ≥95% relative to that seen in control siRNA-transfected cells. Prior knockdown of TRAF6 completely blocked LPS-induced SFK activation compared with the control siRNA-transfected cells (Fig. 3*B*). Infection of HMVEC-Ls with increasing m.o.i. of Ad-TRAF6-DN resulted in dose-dependent overexpression of FLAG-tagged TRAF6-DN (Fig. 3*C*) that inhibited LPS-induced SFK activation >80% compared with that seen in the Ad-null controls (Fig. 3, *D* and *E*). Finally, preincubation of HMVEC-Ls with the cell-permeable TRAF6-targeting peptide diminished SFK activation in response to the LPS stimulus >50% compared with that seen in cells treated with either the SP (Fig. 3*F*) or TRAF6 P3A (data not shown). Taken together, these combined data indicate that TRAF6 is required for SFK activation in HMVEC-Ls in response to LPS and that the proline-rich sequence in TRAF6 (aa 461–469) is necessary for signal transduction.

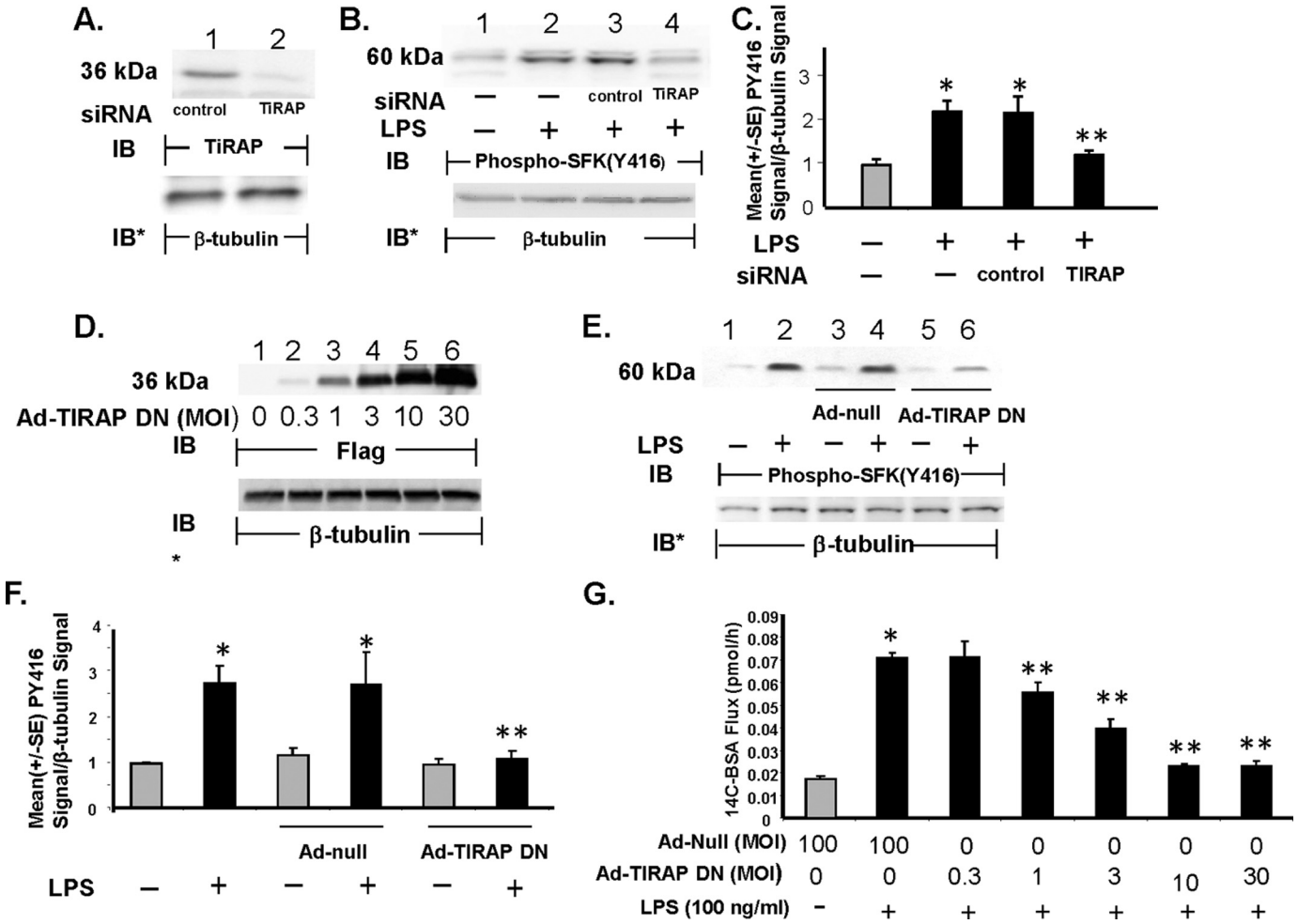

FIGURE 1. **Requirement for TIRAP/Mal for LPS-induced SFK activation and barrier disruption.** *A,* HMVEC-Ls were transfected with TIRAP targeting or control siRNAs and after 48 h were lysed and the lysates processed for TIRAP immunoblotting (*IB*). *B,* HMVEC-Ls transfected with TIRAP targeting or control siRNAs were exposed for 15 min to LPS (300 ng/ml) or medium alone and lysed, and the lysates were processed for phospho-SFK (Tyr^{416}) immunoblotting ($n = 3$). *D,* HMVEC-Ls were transiently infected with increasing m.o.i. of Ad encoding for a FLAG-tagged DN TIRAP/Mal and lysed, and the lysates were processed for FLAG immunoblotting. This blot is representative of two independent experiments. *E,* HMVEC-Ls transiently infected with Ad-TIRAP DN (m.o.i. = 30) or Ad-null (m.o.i. = 100) were incubated for 15 min with LPS (100 ng/ml) or medium alone and processed for phospho-SFK (Tyr^{416}) immunoblotting ($n = 3$). *A, B, D,* and *E,* to control for protein loading and transfer, the blots were stripped and reprobed for β-tubulin. *IB,* immunoblot. *IB*,* immunoblot after strip and reprobe. *C* and *F,* for each immunoblot generated in *B* and *E*, respectively, densitometric quantification of each phospho-SFK (Tyr^{416}) signal was normalized to β-tubulin signal in the same lane in the same blot. *Vertical bars* represent mean (±S.E.) arbitrary densitometry units of phospho-SFK signal normalized to arbitrary densitometry units of β-tubulin signal. ($n = 3$). *G,* HMVEC-Ls cultured in barrier assay chambers were transiently infected with increasing m.o.i. (0.3–30) of Ad-TIRAP DN or Ad-null (m.o.i. = 100), and after 48 h, base-line barrier function for each monolayer was established. Monolayers were then incubated for 6 h with LPS (100 ng/ml) or medium alone and again assayed for transendothelial [^{14}C]BSA flux. *Vertical bars* represent mean (±S.E.) transendothelial [^{14}C]albumin flux in pmol/h immediately following the 6-h study period. *n*, the number of monolayers studied, is six for all groups. *, significantly increased compared with the simultaneous medium control at $p < 0.05$. **, significantly decreased compared with the LPS-exposed control siRNA-transfected or Ad-null infected monolayers at $p < 0.05$.

LPS Increases TRAF6 Association with c-Src—Because the data in Fig. 3 clearly demonstrate that TRAF6 is required for LPS-induced SFK activation, we used an *in vitro* GST-TRAF6 binding assay to establish whether TRAF6 associates with c-Src upon LPS stimulation. When lysates of LPS-treated and medium control HMVEC-Ls were incubated with WT GST-TRAF6 immobilized on glutathione-Sepharose beads, LPS, at >50 ng/ml, dose-dependently increased binding of c-Src to WT TRAF6 (Fig. 4*A*). LPS exposure times of 3–30 min increased the interaction between WT TRAF6 and c-Src with maximal association observed at 3 and 15 min (Fig. 4*B*, *lanes 3, 5,* and *7*). However, when these same lysates from LPS-treated and medium control HMVEC-Ls were incubated with a GST fusion protein of mutated TRAF6, in which the three prolines within the putative SH3-binding motif were each substituted with an alanine, *i.e.* TRAF6 P3A, the LPS-induced increases in TRAF6-c-Src association were profoundly diminished compared with TRAF6 association with WT TRAF6 (Fig. 4*B*, *lanes 2, 4,* and *6*). To ensure that these Pro → Ala substitutions did not compromise overall TRAF6 structural integrity, IRAK1 binding to the mutated GST-TRAF6 P3A was also assessed (Fig. 4*C*). Although the putative SH3-binding motif was disrupted, LPS still increased IRAK1 association with the mutated TRAF6. Finally, preincubation of the lysates of LPS-stimulated cells with the cell-permeable TRAF6 decoy peptide that corresponds to this same proline-rich motif in TRAF6 inhibited binding of c-Src (*lane 3*) compared with lysates preincubated with the control peptide SP (*lane 4*, Fig. 4*D*). Collectively, our findings

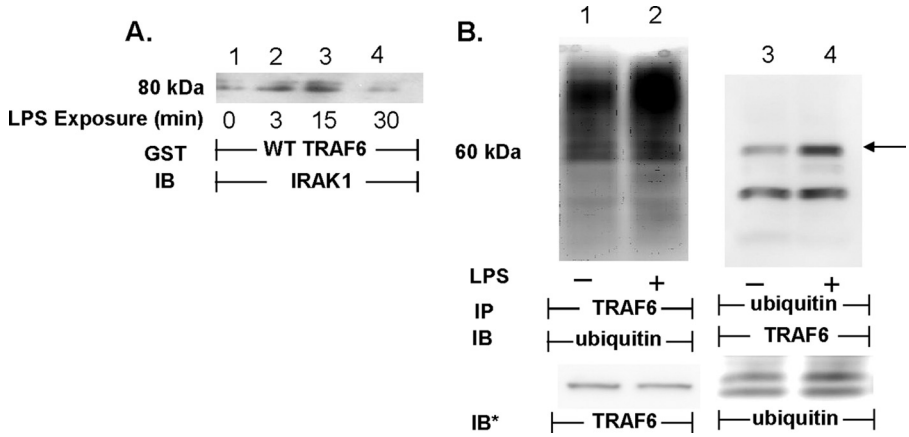

FIGURE 2. **LPS activates TRAF6 in HMVEC-Ls.** *A,* HMVEC-Ls were incubated for increasing times with LPS (300 ng/ml) or medium alone, and lysates were incubated with WT GST-TRAF6 immobilized on glutathione-Sepharose beads. TRAF6-binding proteins were processed for IRAK1 immunoblotting. *B,* HMVEC-Ls were incubated for 15 min with LPS (300 ng/ml) (*lanes 2* and *4*) or medium alone (*lanes 1* and *3*) and lysed, and the lysates were immunoprecipitated with either anti-TRAF6 (*lanes 1* and *2*) or anti-ubiquitin (*lanes 3* and *4*) antibodies. The TRAF6 immunoprecipitates were processed for ubiquitin immunoblotting, whereas the polyubiquitinated immunoprecipitates were processed for TRAF6 immunoblotting. To control for efficiency of immunoprecipitation, protein loading, and transfer, the blots were stripped and reprobed with the immunoprecipitating antibody. Molecular mass in kDa is indicated on *left*. *Arrow* on *right* indicates bands of interest. *IP,* immunoprecipitate. *IB,* immunoblot. *IB**, immunoblot after strip and reprobe. Each of these blots is representative of ≥2 independent experiments.

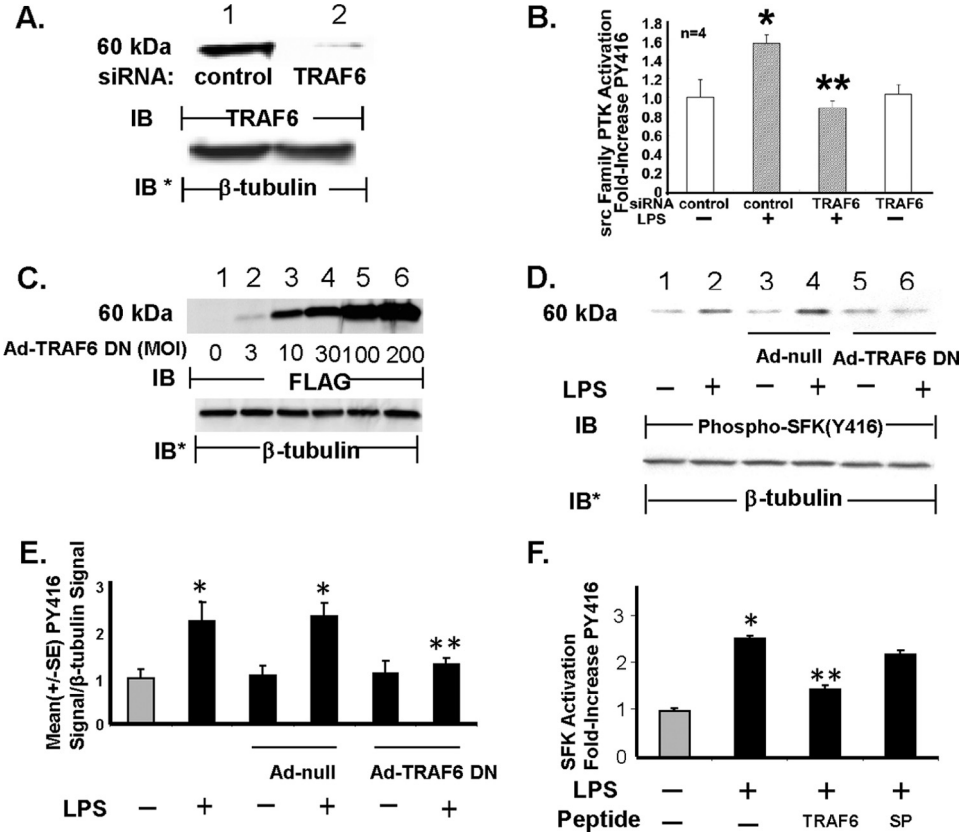

FIGURE 3. **TRAF6 required for SFK activation.** HMVEC-Ls were transfected with TRAF6-targeting or control siRNA, and after 48 h they were processed for immunoblotting to detect TRAF6 protein (*A*) or after exposure to LPS (100 ng/ml) or medium alone a cell-based ELISA to detect SFK Tyr^{416} phosphorylation ($n = 4$) (*B*). *C,* HMVEC-Ls transiently infected with increasing m.o.i. of Ad encoding for a FLAG-tagged TRAF6 DN were lysed and the lysates processed for FLAG immunoblotting. This blot is representative of two independent experiments. *D,* HMVEC-Ls infected with Ad-TRAF6 DN or Ad-null (m.o.i. = 100) were treated for 15 min with LPS (100 ng/ml) or medium alone, after which the cells were lysed and the lysates processed for phospho-SFK (Tyr^{416}) immunoblotting ($n = 3$). *A, C,* and *D*, to control for protein loading and transfer, blots were stripped and reprobed for β-tubulin. *A, C,* and *D*, *IB,* immunoblot; *IB**, immunoblot after strip and reprobe. *E,* for each immunoblot generated in *D*, densitometric quantification of each phospho-SFK (Tyr^{416}) signal was normalized to β-tubulin signal in the same lane in the same blot. *Vertical bars* represent mean (±S.E.) arbitrary densitometry units of phospho-SFK signal normalized to arbitrary densitometry units of β-tubulin signal ($n = 3$). *F,* HMVEC-Ls were preincubated with cell-permeable TRAF6 decoy peptide or SP, after which they were exposed for 15 min to LPS (300 ng/ml) or medium alone, and the cells were processed for the cell-based ELISA to detect SFK Tyr(P)^{416} ($n = 9$). * indicates significantly increased compared with the medium or siRNA control at $p < 0.05$. ** indicates significantly decreased compared with LPS + the control siRNA, Ad-null infected controls, or the control peptide at $p < 0.05$.

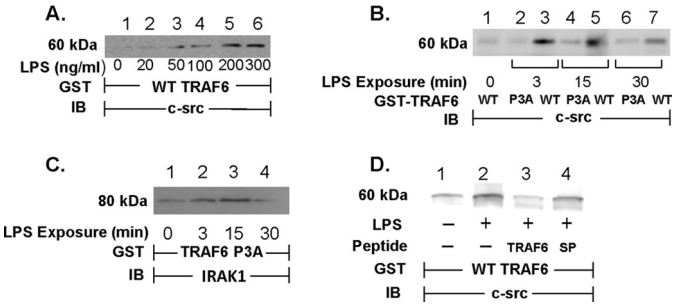

FIGURE 4. **LPS increases association of c-Src with TRAF6.** HMVEC-Ls were transiently infected with Ad-c-Src (m.o.i. = 200) and cultured for 48 h. *A,* c-Src-overexpressing HMVEC-Ls were incubated for 15 min with increasing concentrations of LPS or medium alone. *B* and *C,* HMVEC-Ls overexpressing c-Src were incubated for increasing times to LPS (300 ng/ml) or medium alone. *D,* HMVEC-Ls overexpressing c-Src were preincubated for 0.5 h with the TRAF6 decoy peptide (40 μM), SP (40 μM), or medium alone, after which they were treated for 15 min with LPS (300 ng/ml) or medium alone. Cell lysates in *A* and *D* were incubated with WT GST-TRAF6 immobilized on glutathione-Sepharose beads. *B*, lysates were incubated with either immobilized WT GST-TRAF6 or GST-TRAF6 P3A. *C,* lysates were incubated with immobilized GST-TRAF6 P3A. The TRAF6-binding proteins bound to the beads were processed for immunoblotting (*IB*) in *A, B,* and *D* for c-Src and in *C* for IRAK1. Each blot is representative of ≥2 experiments.

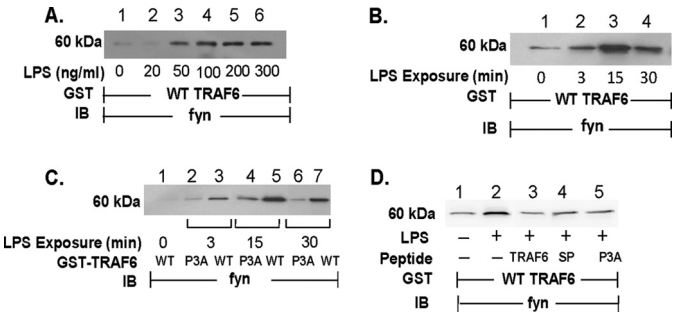

FIGURE 5. **LPS increases association of Fyn with TRAF6.** HMVEC-Ls were transiently infected with Ad-Fyn (m.o.i. = 200) and cultured for 48 h. *A,* HMVEC-Ls overexpressing Fyn were incubated for 15 min with increasing concentrations of LPS or medium alone. *B* and *C*, HMVEC-Ls overexpressing Fyn were incubated for increasing times to LPS (300 ng/ml) or medium alone. *D,* HMVEC-Ls overexpressing Fyn were preincubated for 0.5 h with the TRAF6-targeting peptide or either of two control peptides (40 μM), after which the cells were treated for 15 min with LPS (300 ng/ml) or medium alone. Cells were lysed, and the lysates were incubated with WT GST-TRAF6 immobilized on beads in *A–D* and with immobilized GST-TRAF6 P3A in *C*. In all cases, the TRAF6-binding proteins bound to the beads were processed for Fyn immunoblotting (*IB*). Each blot is representative of ≥2 experiments.

indicate that over the same time period that LPS activates TRAF6 and c-Src, these two molecules physically interact and that the proline-rich motif in TRAF6 is required for the interaction.

LPS Increases TRAF6 Association with Fyn—In non-EC systems, TRAF6 has been reported to interact with c-Src in response to IL-1 and ligands for members of the TNF receptor superfamily (27–31). We now have extended this finding to the EC response to LPS (Fig. 4). In HMVEC-Ls, LPS not only activates c-Src but other SFKs as well, including Fyn (5). Accordingly, we asked whether LPS stimulation might also increase TRAF6 association with Fyn. When lysates of LPS-treated and medium control HMVEC-Ls were incubated with WT GST-TRAF6, LPS dose- (Fig. 5*A*) and time- (Fig. 5*B*) dependently increased binding of Fyn to TRAF6. These changes in TRAF6-Fyn association occurred upon stimulation with the identical LPS doses and exposure times that elicited TRAF6-c-Src association (Fig. 4, *A* and *B*). As was observed with c-Src, disruption of the proline-rich putative SH3-binding motif in TRAF6 profoundly diminished the TRAF6-Fyn interaction (Fig. 5*C, lanes 2, 4,* and *6*). Finally, preincubation of the lysates of LPS-stimulated cells with the cell-permeable TRAF6 decoy peptide diminished binding of Fyn (*lane 3*) compared with lysates preincubated with the scrambled and mutated control peptides (*lanes 4* and *5*, respectively; Fig. 5*D*). These findings indicate that upon LPS stimulation, the TRAF6-SFK interaction can be extrapolated to SFKs other than c-Src, specifically Fyn, and that again an intact proline-rich putative SH3-binding motif in TRAF6 is required for this interaction.

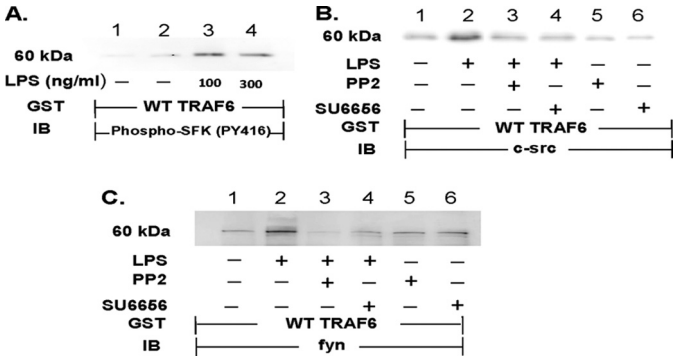

FIGURE 6. **SFK catalytic activity required for SFK-TRAF6 association.** HMVEC-Ls were transiently infected with either Ad-c-Src (m.o.i. = 200) or Ad-Fyn (m.o.i. = 200) and cultured for 48 h. *A,* SFK-overexpressing HMVEC-Ls were incubated for 15 min with LPS (100 ng/ml) or medium alone and lysed, and the lysates were incubated with WT GST-TRAF6 immobilized on beads. The TRAF6-binding proteins were processed for activated phospho-SFK (Tyr(P)^{416}) immunoblotting (*IB*). *B* and *C,* after preincubation with PP2 (10 μM), SU6656 (5 μM), or medium alone, the cells were treated for 15 min with LPS (300 ng/ml) or medium alone, and the cell lysates incubated with WT GST-TRAF6 immobilized on beads. The TRAF6-binding proteins that bound to the beads were processed for c-Src (*B*) or Fyn (*C*) immunoblotting. Each blot is representative of ≥2 experiments.

SFK Catalytic Activity Required for SFK-TRAF6 Association—In HMVEC-Ls, LPS stimulation of TLR4 activates multiple SFKs (5) and increases their association with TRAF6 (Figs. 4 and 5). To determine whether activated SFKs bind TRAF6, lysates of LPS-treated and medium control HMVEC-Ls were incubated with GST-WT TRAF6 and the TRAF6-binding proteins processed for phospho-SFK (Tyr(P)^{416}) immunoblotting (Fig. 6*A*). LPS increased association of activated Tyr(P)^{416}-containing SFK (Fig. 6*A, lanes 3* and *4*) compared with medium controls (*lanes 1* and *2*). To establish whether the catalytic state of SFKs regulate their interaction with TRAF6, HMVEC-Ls were preincubated with either of two SFK-selective tyrosine kinase inhibitors, PP2 and SU6656, after which they were treated with LPS or medium alone. When the HMVEC-L lysates were incubated with WT GST-TRAF6, LPS increased association of either c-Src (Fig. 6*B*, *lane 2*) or Fyn (Fig. 6*C*, *lane 2*) to TRAF6, and prior SFK-selective inhibition completely blocked this association (Fig. 6, *B*, *lanes 3* and *4,* and *C*, *lanes 3* and *4*). These data indicate that the SFK molecule must be in the catalytically active, open conformation when it binds to TRAF6.

TRAF6 Catalyzes Lys^{63}-linked Ubiquitination of SFKs—TRAF6 is not only an autocatalytic Lys^{63} ubiquitin ligase (27, 34, 36, 37) but also catalyzes Lys^{63}-linked ubiquitination of

other signaling molecules (44, 45). The MATH domain of TRAF6 contains a proline-rich sequence that is required for its physical association with either c-Src (Fig. 4*B*) (27, 31) or Fyn (Fig. 5*C*). Although the COOH-terminal MATH domain is sufficient for the TRAF6-SFK interaction, alone it cannot support SFK activation (31), implying that sequences NH_2-terminal to this domain are operative in the regulation of SFK catalytic activity. It is within the NH_2-terminal RING domain and the first zinc finger region that the Lys^{63} ubiquitin ligase activity resides (37). Because this same NH_2-terminal domain is required for SFK activation, we asked whether LPS might increase Lys^{63}-linked ubiquitination of one or more SFKs and whether such SFK ubiquitination might be mediated through TRAF6 ubiquitin ligase activity (Fig. 7). LPS increased Lys^{63}-linked ubiquitination of both c-Src (*lanes 4 versus 3*) and Fyn (*lanes 2 versus 1*, Fig. 7*A*). Furthermore, prior silencing of TRAF6 dramatically reduced LPS-stimulated Lys^{63}-linked ubiquitination of both c-Src (90% protection) (*lanes 8 versus 6*) and Fyn (>60% protection) (*lanes 4 versus 2*, Fig. 7*B*). In addition, overexpression of TRAF6-DN, a TRAF6 deletion mutant missing the NH_2-terminal domain that contains its Lys^{63} ubiquitin ligase activity, almost completely blocked Lys^{63}-linked ubiquitination of Fyn (*lanes 6 versus 4* and *2*, Fig. 7, *C* and *D*). Finally, preincubation of HMVEC-Ls with the cell-permeable TRAF6 decoy peptide diminished Lys^{63}-linked ubiquitination of both Fyn (*lane 4*) and c-Src (*lane 8*) by >92% in response to LPS compared with cells preincubated with the P3A control peptide (*lanes 3* and *7*, Fig. 7, *E* and *F*). These data indicate that

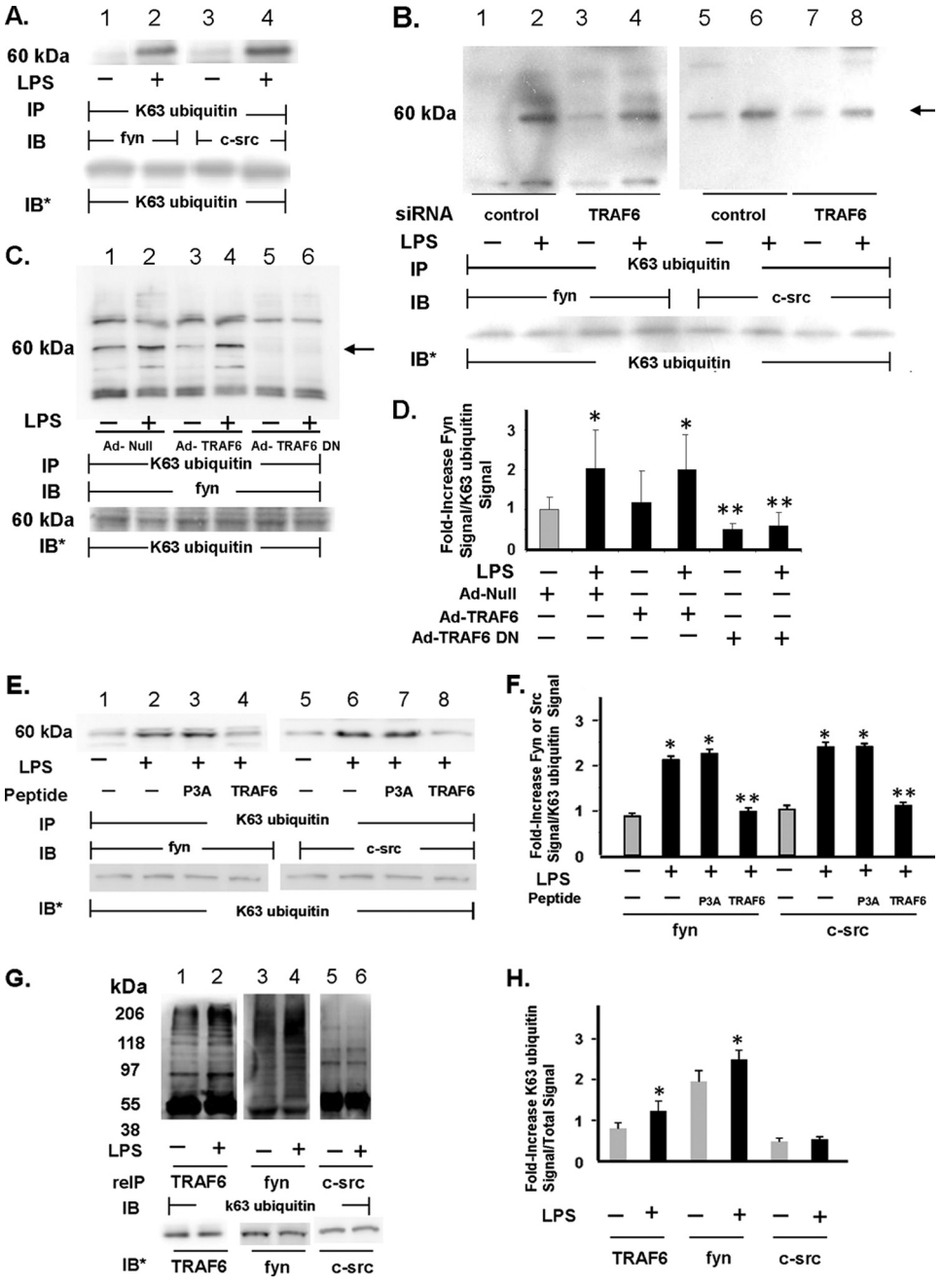

physical association between TRAF6 and SFKs is required for TRAF6-mediated Lys^{63}-linked ubiquitination of Fyn or c-Src. We now have demonstrated that TRAF6 associates with both c-Src (Fig. 4) and Fyn (Fig. 5); TRAF6 is an autocatalytic Lys^{63} ubiquitin ligase (27, 34, 36, 37), and TRAF6 and SFKs share almost identical gel mobilities (Figs. 7*A* and 8*A*). Therefore, it is possible that the bands revealed in the SFK immunoblots (Fig. 7, *A*, *lanes 2* and *4*, *B*, *lanes 2* and *6*, and *C*, *lanes 2* and *4*) could represent nonubiquitinated SFKs that have coimmunoprecipitated with Lys^{63}-linked autoubiquitinated TRAF6. To help address this possibility, TRAF6, Fyn, and c-Src immunoprecipitates were resuspended in 2% SDS, and after dilution, the disrupted complexes were again immunoprecipitated with the same anti-TRAF6, anti-Fyn, and anti-c-Src antibodies and the immunoprecipitates processed for Lys^{63}-specific ubiquitin immunoblotting (Fig. 7, *G* and *H*). Using this re-immunoprecipitation strategy, we found that LPS increased Lys^{63}-linked ubiquitination of Fyn (*lanes 4 versus 3*) but not of c-Src (*lanes 6 versus 5*, Fig. 7*G*). Taken together, these data indicate that in HMVEC-Ls, LPS activates TRAF6, which in turn catalyzes Lys^{63}-linked ubiquitination of the SFK, Fyn, and possibly c-Src. To our knowledge, this is the first report of Lys^{63}-linked ubiquitination of one or more SFKs. Whether this TRAF6-mediated SFK ubiquitination is direct or indirect and/or regulates the catalytic state of one or more SFKs is unknown.

SFK(s) Increases Tyrosine Phosphorylation of TRAF6—LPS stimulation through TLR4 increases the association of SFKs with TRAF6 (Figs. 4 and 5), and an active catalytic state for SFK is required for this association (Fig. 6). Furthermore, during this association, TRAF6 catalyzes Lys^{63}-linked ubiquitination of Fyn and possibly c-Src (Fig. 7). Because TRAF6 contains 12 tyrosine residues, we hypothesized that during the SFK-TRAF6 interaction, SFKs might tyrosine-phosphorylate TRAF6. LPS stimulation of HMVEC-Ls increased tyrosine phosphorylation of TRAF6 (Fig. 8*A*, *lanes 2 versus 1*) that was blocked by prior SFK inhibition (Fig. 8, *B, lanes 4* and *6 versus 2,* and *C*). Preincubation of HMVEC-Ls with the cell-permeable TRAF6 decoy peptide blocked LPS-induced tyrosine phosphorylation of TRAF6 by 78.5% (*lane 3*) compared with the control P3A peptide that had no inhibitory effect (*lane 4,* Fig. 8, *D* and *E*. These results indicate that the SFK-TRAF6 association is a prerequisite for SFK-mediated tyrosine phosphorylation of TRAF6. Again, c-Src and Fyn both associate with TRAF6 (Figs. 4 and 5), and upon activation, each autophosphorylates on Tyr^{416} (6, 7). Because TRAF6 and SFKs share similar gel mobilities, the phosphotyrosine signal associated with the TRAF6 immunoprecipitate (Fig. 8, *A*, *lane 2,* and *B*, *lane 2*) could be explained by coimmunoprecipitated SFK. To discriminate between TRAF6 and associated SFK(s), the TRAF6 immunoprecipitates were disrupted with SDS and re-immunoprecipitated with the anti-TRAF6 antibody (Fig. 8, *F* and *G*). Using the re-immunoprecipitation protocol, tyrosine phosphorylation of TRAF6 was again found to be increased by LPS. To our knowledge, this is the first report of TRAF6 tyrosine phosphorylation. Taken together, our findings suggest that during the TRAF6-SFK association, each binding partner can serve as a substrate for the catalytic activity of the other. Whether these modifications influence binding affinity and/or catalytic activity of either or both proteins is unknown.

TRAF6 Required for LPS-induced Barrier Disruption—Having established that TRAF6 is required for LPS-induced SFK activation (Fig. 3), that SFK activation is required for its association to TRAF6 (Fig. 6), and having previously found that SFK activation is a prerequisite to LPS-induced endothelial barrier dysfunction (5), we evaluated whether TRAF6 might also be necessary for LPS-induced barrier disruption. TRAF6 was again targeted in a barrier assay with three distinct interventions as follows: 1) siRNA-induced silencing of TRAF6; 2) overexpression of TRAF6 DN, and finally 3) preincubation with a cell-permeable TRAF6-specific decoy peptide. Prior knockdown of TRAF6 protected against LPS-induced increases in transendothelial [^{14}C]BSA flux by 70% compared with that seen across control siRNA-transfected monolayers (Fig. 9*A*). Overexpression of TRAF6 DN dose-dependently diminished the LPS-induced increases in albumin flux, and at an m.o.i. = 100, it protected against the increase by >76% compared with that

FIGURE 7. **TRAF6 catalyzes Lys^{63}-linked ubiquitination of SFKs.** *A,* HMVEC-Ls were treated for 0.5 h with LPS (300 ng/ml) or medium alone and lysed, and the lysates were immunoprecipitated with antibody that specifically recognizes Lys^{63}-linked ubiquitin chains. The Lys^{63}-specific ubiquitin immunoprecipitates were processed for c-Src (*lanes 3* and *4*) or Fyn (*lanes 1* and *2*) immunoblotting. *B,* HMVEC-Ls transfected with TRAF6-targeting or control siRNAs were treated for 0.5 h with LPS (300 ng/ml) or medium alone, and the cell lysates were immunoprecipitated with anti-Lys^{63}-specific ubiquitin antibodies. The immunoprecipitates were processed for c-Src (*lanes 5–8*) or Fyn (*lanes 1–4*) immunoblotting. *C,* HMVEC-Ls transiently infected with Ad-null, Ad-TRAF6, or Ad-TRAF6 DN (m.o.i. = 100) were treated for 0.5 h with LPS (300 ng/ml) or medium alone and lysed, and the lysates were immunoprecipitated with anti-Lys^{63}-specific ubiquitin antibodies. The immunoprecipitates were processed for Fyn immunoblotting. *D,* for each immunoblot generated in *C*, densitometric quantitation of each Lys^{63}-linked ubiquitinated Fyn signal was normalized to Lys^{63} ubiquitin signal in the same lane in the same blot. *Vertical bars* represent mean (±S.E.) arbitrary densitometry units of Lys^{63}-linked ubiquitinated Fyn signal normalized to arbitrary densitometry units of Lys^{63} ubiquitin signal ($n \geq 4$). *E,* HMVEC-Ls were preincubated with cell-permeable TRAF6 decoy peptide or the control P3A peptide, after which they were exposed for 15 min to LPS (300 ng/ml) or medium alone and lysed, and the lysates were immunoprecipitated with anti-Lys^{63}-specific ubiquitin antibodies. The immunoprecipitates were processed for c-Src (*lanes 5–8*) or Fyn (*lanes 1–4*) immunoblotting. *F,* for each immunoblot generated in *E*, densitometric quantitation of each Lys^{63}-linked ubiquitinated Fyn/c-Src signal was normalized to Lys^{63} ubiquitin signal in the same lane in the same blot. *Vertical bars* represent mean (±S.E.) arbitrary densitometry units of Lys^{63}-linked ubiquitinated SFK signal normalized to arbitrary densitometry units of Lys^{63} ubiquitin signal ($n = 3$). *G,* lysates of LPS-treated and medium control HMVEC-Ls were immunoprecipitated with anti-TRAF6, anti-Fyn, and anti-c-Src antibodies. The immune complexes were resuspended in 2% SDS, heat-treated, and again immunoprecipitated with the same anti-TRAF6, anti-Fyn, and anti-c-Src antibodies. The immunoprecipitates were processed for Lys^{63}-specific ubiquitin immunoblotting. *H,* for each immunoblot generated in *G,* densitometric quantitation of each Lys^{63}-linked ubiquitin signal associated with each TRAF6, Fyn, and c-Src immunoprecipitate was normalized to the total TRAF6, Fyn, and c-Src signals, respectively, in the same lane in the same blot. *Vertical bars* represent mean (±S.E.) arbitrary densitometry units of Lys^{63}-specific ubiquitin signal for TRAF6, Fyn, and c-Src normalized to arbitrary densitometry units of total TRAF6, Fyn, and c-Src signals, respectively ($n = 3$). *, significantly increased compared with the simultaneous medium control at $p < 0.05$. **, significantly decreased compared with the LPS-exposed Ad-TRAF6 infected or P3A control peptide treated HMVEC-Ls at $p < 0.05$. *A–C, E,* and *G*, to control for protein loading and transfer, blots were stripped and reprobed with the immunoprecipitating antibody. Molecular mass in kDa is indicated on *left. B* and *C*, *arrow* on *right* indicates bands of interest. *IP,* immunoprecipitate; *reIP,* re-immunoprecipitate; *IB,* immunoblot; *IB**, immunoblot after strip and reprobe. Each blot is representative of two independent experiments.

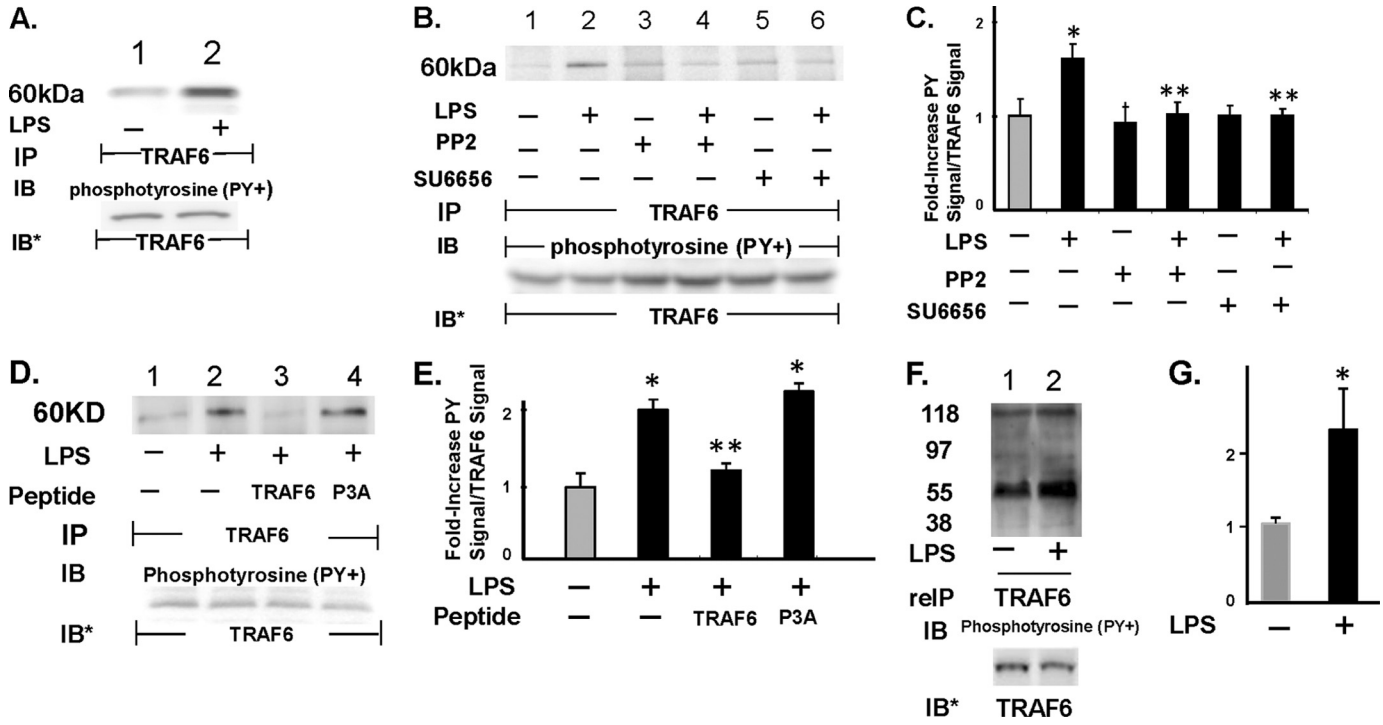

FIGURE 8. **SFK(s) increases tyrosine phosphorylation of TRAF6.** *A,* HMVEC-Ls were treated for 0.5 h with LPS (300 ng/ml) or medium alone, and the cell lysates were immunoprecipitated with anti-TRAF6 antibodies. The TRAF6 immunoprecipitates were processed for phosphotyrosine immunoblotting. *B,* HMVEC-Ls preincubated with either PP2 or SU6656 were similarly treated with LPS or medium alone, after which they were lysed, and the lysates were processed for TRAF6 immunoprecipitation followed by phosphotyrosine immunoblotting. *C,* for each immunoblot generated in *B*, densitometric quantitation of each Tyr(P)-TRAF6 signal was normalized to total TRAF6 signal in the same lane in the same blot. *Vertical bars* represent mean (±S.E.) arbitrary densitometry units of Tyr(P)-TRAF6 signal normalized to arbitrary densitometry units of total TRAF6 signal ($n \geq 4$). *D,* HMVEC-Ls were preincubated with cell-permeable TRAF6 decoy peptide or the P3A control peptide, after which they were exposed for 15 min to LPS (300 ng/ml) or medium alone and lysed, and the lysates were immunoprecipitated with anti-TRAF6 antibodies. The TRAF6 immunoprecipitates were processed for phosphotyrosine immunoblotting. *E,* for each immunoblot generated in *D*, densitometric quantitation of each phospho-TRAF6 signal was normalized to total TRAF6 signal in the same lane in the same blot. *Vertical bars* represent mean (±S.E.) arbitrary densitometry units of phospho-TRAF6 signal normalized to arbitrary densitometry units of total TRAF6 signal ($n = 3$). *F,* lysates of LPS-treated and medium control HMVEC-Ls were immunoprecipitated with anti-TRAF6 antibodies after which the immune complexes were resuspended in 2% SDS, heat-treated, and again immunoprecipitated with the same anti-TRAF6 antibody, and the TRAF6 immunoprecipitates were processed for phosphotyrosine immunoblotting. *G,* for each immunoblot generated in *F*, densitometric quantitation of each Tyr(P)-TRAF6 signal was normalized to total TRAF6 signal in the same lane in the same blot. *Vertical bars* represent mean (±S.E.) arbitrary densitometry units of Tyr(P)-TRAF6 signal normalized to arbitrary densitometry units of total TRAF6 signal ($n = 3$). *, significantly increased compared with the simultaneous medium control at $p < 0.05$. **, significantly decreased compared with the LPS-treated HMVEC-Ls at $p < 0.05$. *A, B, D,* and *F,* to control for efficiency of immunoprecipitation and protein loading and transfer, blots were stripped and reprobed with the immunoprecipitating antibody. *IP,* immunoprecipitate; *relP,* reimmunoprecipitated; *IB,* immunoblot; *IB**, immunoblot after stripping and reprobe. Molecular mass in kDa is indicated on *left*. Each blot is representative of ≥3 independent experiments.

seen in Ad-null-infected monolayers (Fig. 9*B*). Finally, preincubation with the TRAF6-specific decoy peptide completely protected against LPS-induced barrier disruption compared with that measured across monolayers pretreated with control SP (Fig. 9*C*). These combined data indicate that TRAF6 activation is required for full expression of endothelial barrier disruption in response to LPS.

DISCUSSION

In this study, we have established the absolute requirement for TRAF6 in HMVEC-Ls for LPS-induced SFK activation (Fig. 3) and barrier disruption (Fig. 9). In HMVEC-Ls, LPS increases TRAF6 polyubiquitination and its association with IRAK1 (Fig. 2). Furthermore, LPS increased TRAF6 association with each of two SFKs, c-Src (Fig. 4) and Fyn (Fig. 5), and this TRAF6-SFK association required both an intact proline-rich putative SH3-binding motif in TRAF6 (Figs. 4*B* and 5*C*) and a catalytically active state in the SFKs (Fig. 6). TRAF6-catalyzed Lys^{63}-linked ubiquitination of Fyn and possibly c-Src (Fig. 7) and SFK(s) increased tyrosine phosphorylation of TRAF6 (Fig. 8). Together, these data establish TRAF6 as the pivotal signaling molecule that couples LPS engagement of TLR4 to SFK activation and loss of endothelial barrier integrity.

TLR4 activation can transduce signals downstream through both MyD88-dependent and MyD88-independent signaling pathways (12, 15, 18). In the MyD88-dependent pathway, recruitment of MyD88 to the TLR4 signaling complex is facilitated by the bridging adapter molecule, TIRAP/Mal (15). TIRAP/Mal also contains a putative TRAF6-binding motif that enables it to interact directly with and recruit TRAF6 transiently to the plasma membrane (46, 47). TIRAP/Mal is central to the MyD88-dependent pathway in the cases of TLR2 and TLR4. That either prior knockdown of TIRAP/Mal or overexpression of a TIRAP/Mal DN in HMVEC-Ls protected against LPS-induced SFK activation and barrier disruption (Fig. 1) indicates that these LPS-induced EC responses require an intact MyD88-dependent pathway. The MyD88-independent TLR4 signaling pathway utilizes another bridging adapter, TRAM, to recruit TRIF (also referred to as TICAM-1) to TLR4 (12, 15, 18). Recently, in a yeast two-hybrid system, the NH_2-terminal por-

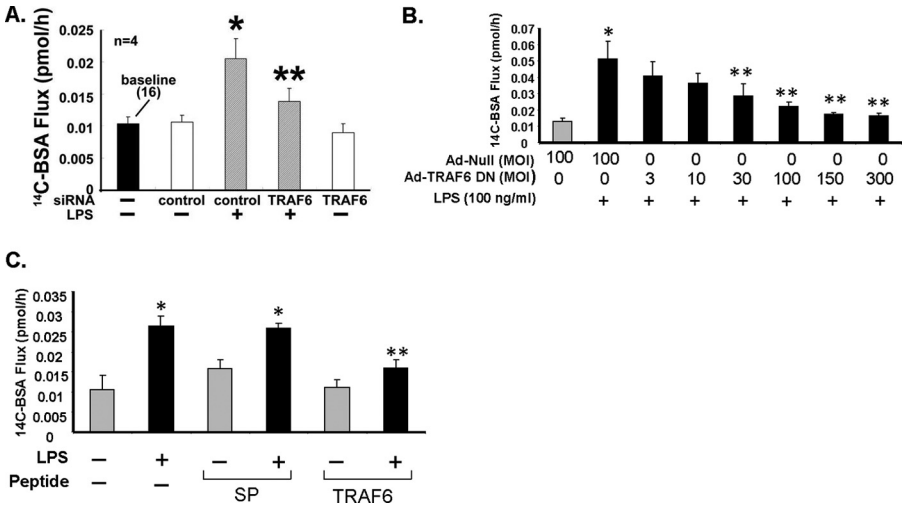

FIGURE 9. **TRAF6 required for endothelial barrier response to LPS.** *A,* HMVEC-L monolayers transfected with TRAF6-targeting or control siRNAs were cultured to postconfluence in barrier assay chambers after which base-line barrier function was established ($n = 4$). *B,* HMVEC-Ls cultured in assay chambers were transiently infected with increasing m.o.i. of Ad-TRAF6 DN or Ad-null (m.o.i. = 100) ($n = 6$) and cultured to postconfluence. *C,* postconfluent HMVEC-L monolayers were preincubated for 0.5 h with TRAF6 decoy or control SP (40 μM) ($n = 6$). *A–C,* the monolayers were treated for 6 h with LPS (100 ng/ml) or medium alone, after which transendothelial [^{14}C]BSA flux was assayed. *Vertical bars* represent mean (±S.E.) transendothelial [^{14}C]BSA flux in pmol/h immediately following the 6-h study period. *, significantly increased compared with the simultaneous control siRNA alone (*A*) and medium control (*B* and *C*) all at $p <$ 0.05. **, significantly decreased compared with control siRNA + LPS (*A*), Ad-null + LPS (*B*), and control peptide + LPS (*C*), all at $p < 0.05$.

tion of TRIF was shown to interact with the COOH terminus of TRAF6, and abrogation of this interaction strongly inhibited TRIF-mediated interferon-β induction (48). Although our data establish both LPS-induced SFK activation and barrier disruption as TIRAP/Mal-dependent, thereby implicating involvement of the MyD88-dependent pathway, in these studies, participation of the TRIF-dependent pathway has not been formally excluded.

The NH_2-terminal RING domain of TRAF6 is an E3 ubiquitin ligase that, in concert with the dimeric E2 enzyme Ubc/Uev1A, catalyzes its own autoubiquitination via site-specific Lys^{63}-linked polyubiquitin chains (22, 23). TRAF6 autoubiquitination is a prerequisite to selected downstream signaling events, including IκB kinase and MAPK activation (22, 23). Whether TRAF6 autoubiquitination is required for its association with SFKs was unknown. Because LPS increased SFK association with unmodified *E. coli*-derived GST-TRAF6 (Figs. 4 and 5), TRAF6 ubiquitination is clearly not required for this interaction. When our prokaryote-generated GST-TRAF6 was processed for ubiquitin immunoblotting, as anticipated, ubiquitin could not be detected.[4] TRAF6 also has been reported to catalyze Lys^{63}-linked ubiquitination of other signaling molecules such as AKT (44) and other ubiquitin ligases, including cIAP1 and -2 (45). In several reports, activated SFKs were shown to be ubiquitinated and targeted for degradation by the proteasome (49–51), presumably via Lys^{48}-linked ubiquitination. We asked whether LPS activation of TRAF6 might lead to Lys^{63}-linked ubiquitination of one or more SFKs. In HMVEC-Ls, increased Lys^{63}-linked ubiquitination of Fyn, as detected by re-immunoprecipitation (Fig. 7*G*, *lane 4*) and possibly c-Src (Fig. 7*A*, *lane 4*), was detected in response to LPS. It is conceivable that SDS treatment during re-immunoprecipitation denatured and rendered the anti-c-Src antibody nonimmunogenic. Furthermore, TRAF6 was required for this modification (Fig. 7, *B–D*). Although TRAF6 autoubiquitination may be required under some conditions for multiple signaling events (22, 23, 51–53), this modification does not appear to regulate the TRAF6-SFK interaction. Whether Lys^{63}-linked ubiquitination of SFKs influences either their catalytic state or their association with TRAF6 remains to be determined.

TRAF6 and c-Src have been reported to interact physically in signaling pathways in non-EC systems (27–31). In murine osteoclasts and dendritic cells, TNF-related activation-induced cytokine, also known as RANKL, increased co-immunoprecipitation of c-Src with TRAF6 (31). In these same co-expression studies, an NH_2-terminal deletion mutant, TRAF6(289–530), was sufficient to co-immunoprecipitate c-Src, whereas a COOH-terminal deletion mutant, TRAF6(1–289), could not. The authors found that GST-c-Src-SH3 interacted directly with *in vitro* translated TRAF6, and they mapped the interacting motif in TRAF6 to a proline-rich sequence, aa 461–469 (RPTIPRNPK). When one or more of these prolines was substituted with alanine(s), the TRAF6-c-Src association was disrupted. In murine osteoclast-like cells, the human T98G glioblastoma cell line, and human embryonic kidney HEK293T cells, human recombinant IL-1α also increased TRAF6-c-Src association in coimmunoprecipitation assays (29). Finally, IL-1β increased the association of a fluoroprobe-labeled TRAF6 with labeled c-Src in the cytoplasm of living HEK293 T cells (27). Here, we now have established that the TRAF6-c-Src interaction can be extended to LPS/TLR4 signaling (Fig. 4), to another SFK, Fyn (Fig. 5), and to HMVEC-Ls (Figs. 4 and 5).

Although it is clear that TRAF6 can physically engage SFKs (Figs. 4 and 5) (27–31), the relative hierarchical position between these two signaling elements within any one signaling network is unclear. In this study, we found that prior siRNA-induced silencing of TRAF6 completely blocked SFK activation (Fig. 3*B*), suggesting that TRAF6 is upstream of SFKs.

[4] A. Liu, personal communication.

However, we found that prior pharmacological blockade of SFK activation prevented SFK binding to TRAF6 (Fig. 6, *B* and *C*), suggesting that prior SFK activation is required for its interaction with TRAF6. Activation of SFKs involves autophosphorylation of Tyr^{416} within the activation loop and release from the autoinhibited restrained state (6, 7). Perhaps only in this activated state with its open conformation is the SH3 domain within SFK accessible for binding to the proline-rich putative TRAF6 SH3-binding domain. A number of other studies have addressed this same issue (28–31), yet the hierarchical relationship between TRAF6 and SFKs remains unresolved. In selected experimental systems, overexpression of TRAF6 stimulated SFK activation (31) and SFK-mediated downstream signaling events (27–30). However, in cells of monocyte/macrophage lineage, stimulation of CD40, a member of the TNF receptor superfamily, recruits TRAF6 to the receptor and leads to c-Src activation (30). Preincubation of cells with a cell-permeable peptide that competitively inhibits TRAF6 recruitment and binding to CD40 did not prevent c-Src activation, suggesting that c-Src might be upstream of TRAF6. These combined data generated in various host systems do not conclusively indicate which of the two signaling molecules, TRAF6 or SFK(s), is upstream to the other. In this study, we found that TRAF6 catalyzes Lys^{63}-linked ubiquitination of one or more SFKs, while at the same time, SFKs increase tyrosine phosphorylation of TRAF6. The interaction(s) between TRAF6 and SFKs is likely a complex two-way multistep process in which more than one TRAF6 domain participates and SFKs activate other SFKs.

We now have established TRAF6 as a critical adapter molecule in HMVEC-Ls for LPS/TLR4-induced SFK activation (Fig. 3) and barrier disruption (Fig. 9). Other reports have similarly indicated that TRAF6 is a key mediator of vascular endothelial pathophysiology (54–57). In human dermal microvascular ECs, TRAF6 is required for LPS-induced angiogenesis (54), a multistep process that involves hyperpermeable vessels (58). In fact, TRAF6 has been shown to mediate increased permeability across human umbilical vein EC monolayers in response to both receptor activator of NF-κB ligand (55) and IL-33 (56). In human carotid arteries, TRAF6 expression is increased in atherosclerotic lesions, and silencing of TRAF6 blocks proatherogenic gene expression in human saphenous vein ECs (57). It is conceivable that TRAF6 is a pivotal signaling element in a final common pathway for the host response to a subset of injurious stimuli, including bacterial LPS, for life-threatening vascular leak syndromes.

Acknowledgment—We thank Shirley A. Taylor for excellent secretarial support.

REFERENCES

1. Brigham, K. L., and Meyrick, B. (1986) Endotoxin and lung injury. *Am. Rev. Respir. Dis.* **133,** 913–927
2. Bannerman, D. D., and Goldblum, S. E. (1997) Endotoxin induces endothelial barrier dysfunction through protein tyrosine phosphorylation. *Am. J. Physiol.* **273,** L217–L226
3. Bannerman, D. D., Fitzpatrick, M. J., Anderson, D. Y., Bhattacharjee, A. K., Novitsky, T. J., Hasday, J. D., Cross, A. S., and Goldblum, S. E. (1998) Endotoxin-neutralizing protein protects against endotoxin-induced endothelial barrier dysfunction. (1998) *Infect. Immun.* **66,** 1400–1497
4. Goldblum, S. E., Brann, T. W., Ding, X., Pugin, J., and Tobias, P. S. (1994) Lipopolysaccharide (LPS)-binding protein and soluble CD14 function as accessory molecules for LPS-induced changes in endothelial barrier function, in vitro. *J. Clin. Invest.* **93,** 692–702
5. Gong, P., Angelini, D. J., Yang, S., Xia, G., Cross, A. S., Mann, D., Bannerman, D. D., Vogel, S. N., and Goldblum, S. E. (2008) TLR4 signaling is coupled to SRC family kinase activation, tyrosine phosphorylation of zonula adherens proteins, and opening of the paracellular pathway in human lung microvascular endothelia. (2008) *J. Biol. Chem.* **283,** 13437–13449
6. Engen, J. R., Wales, T. E., Hochrein, J. M., Meyn, M. A., 3rd, Banu Ozkan, S., Bahar, I., and Smithgall, T. E. (2008) Structure and dynamic regulation of Src family kinases. *Cell. Mol. Life Sci.* **65,** 3058–3073
7. Benati, D., and Baldari, C. T. (2008) SRC family kinases as potential therapeutic targets for malignancies and immunological disorders. *Curr. Med. Chem.* **15,** 1154–1165
8. Ingley, E. (2008) Src family kinases. Regulation of their activities, levels, and identification of new pathways. *Biochim. Biophys. Acta* **1784,** 56–65
9. Poltorak, A., He, X., Smirnova, I., Liu, M.Y., Van Huffel, C., Du, X., Birdwell, D., Alejos, E., Silva, M., Galanos, C., Freudenberg, M., Ricciardi-Castagnoli, P., Layton, B., and Beutler, B. (1998) Defective LPS signaling in C3H/HeJ and C57BL/10ScCr mice. Mutations in *Tlr4* gene. *Science* **282,** 2085–2088
10. Lien, E., Means, T. K., Heine, H., Yoshimura, A., Kusumoto, S., Fukase, K., Fenton, M. J., Oikawa, M., Qureshi, N., Monks, B., Finberg, R. W., Ingalls, R. R., and Golenbock, D. T. (2000) Toll-like receptor 4 imparts ligand-specific recognition of bacterial lipopolysaccharide. *J. Clin. Invest.* **105,** 497–504
11. Jin, M. S., and Lee, J. O. (2008) Structures of the toll-like receptor family and its ligand complexes. *Immunity* **29,** 182–191
12. Carpenter, S., and O'Neill, L. A. (2009) Recent insights into the structure of Toll-like receptors and post-translational modifications of their associated signaling proteins. *Biochem. J.* **422,** 1–10
13. O'Neill, L. A., and Bowie, A. G. (2007) The family of five. TIR-domain-containing adaptors in Toll-like receptor signaling. *Nat. Rev. Immunol.* **7,** 353–364
14. Kagan, J. C., and Medzhitov, R. (2006) Phosphoinositide-mediated adaptor recruitment controls Toll-like receptor signaling. *Cell* **125,** 943–955
15. Sheedy, F. J., and O'Neill, L. A. (2007) The Troll in Toll. Mal and Tram as bridges for TLR2 and TLR4 signaling. *J. Leukocyte Biol.* **82,** 196–203
16. Zeisel, M. B., Druet, V. A., Sibilia, J., Klein, J. P., Quesniaux, V., and Wachsmann, D. (2005) Cross-talk between MyD88 and focal adhesion kinase pathways. *J. Immunol.* **174,** 7393–7397
17. Davis, C. N., Tabarean, I., Gaidarova, S., Behrens, M. M., and Bartfai, T. (2006) IL-1β induces a MyD88-dependent and ceramide-mediated activation of Src in anterior hypothalamic neurons. *J. Neurochem.* **98,** 1379–1389
18. Akira, S., and Takeda, K. (2004) Toll-like receptor signaling. *Nat. Rev. Immunol.* **4,** 499–511
19. Keating, S. E., Maloney, G. M., Moran, E. M., and Bowie, A. G. (2007) IRAK-2 participates in multiple toll-like receptor signaling pathways to NFκB via activation of TRAF6 ubiquitination. *J. Biol. Chem.* **282,** 33435–33443
20. Lin, S. C., Lo, Y. C., and Wu, H. (2010) Helical assembly in the MyD88-IRAK4-IRAK2 complex in TLR/IL-1R signaling. *Nature* **465,** 885–890
21. Boch, J. A., Yoshida, Y., Koyama, Y., Wara-Aswapati, N., Peng, H., Unlu, S., and Auron, P. E. (2003) Characterization of a cascade of protein interactions initiated at the IL-1 receptor. *Biochem. Biophys. Res. Commun.* **303,** 525–531
22. Deng, L., Wang, C., Spencer, E., Yang, L., Braun, A., You, J., Slaughter, C., Pickart, C., and Chen, Z. J. (2000) Activation of the IκB kinase complex by TRAF6 requires a dimeric ubiquitin-conjugating enzyme complex and a unique polyubiquitin chain. *Cell* **103,** 351–361
23. Lamothe, B., Besse, A., Campos, A. D., Webster, W. K., Wu, H., and Darnay, B. G. (2007) Site-specific Lys-63-linked tumor necrosis factor receptor-associated factor 6 auto-ubiquitination is a critical determinant of IκB kinase activation. *J. Biol. Chem.* **282,** 4102–4112

24. Dobrovolskaia, M. A., and Vogel, S. N. (2002) Toll receptors, CD14, and macrophage activation and deactivation by LPS. *Microbes Infect.* **4,** 903–914
25. Henneke, P., and Golenbock, D. T. (2002) Innate immune recognition of lipopolysaccharide by endothelial cells. *Crit. Care Med.* **30,** S207–S213
26. Dauphinee, S. M., and Karsan, A. (2006) Lipopolysaccharide signaling in endothelial cells. *Lab. Invest.* **86,** 9–22
27. Wang, K. Z., Wara-Aswapati, N., Boch, J. A., Yoshida, Y., Hu, C. D., Galson, D. L., and Auron, P. E. (2006) TRAF6 activation of PI 3-kinase-dependent cytoskeletal changes is cooperative with Ras and is mediated by an interaction with cytoplasmic Src. *J. Cell Sci.* **119,** 1579–1591
28. Nakamura, I., Kadono, Y., Takayanagi, H., Jimi, E., Miyazaki, T., Oda, H., Nakamura, K., Tanaka, S., Rodan, G. A., and Duong le, T. (2002) IL-1 regulates cytoskeletal organization in osteoclasts via TNF receptor-associated factor 6/c-Src complex. *J. Immunol.* **168,** 5103–5109
29. Funakoshi-Tago, M., Tago, K., Sonoda, Y., Tominaga, S., and Kasahara, T. (2003) TRAF6 and c-SRC induce synergistic AP-1 activation via PI3-kinase-AKT-JNK pathway. *Eur. J. Biochem.* **270,** 1257–1268
30. Mukundan, L., Bishop, G. A., Head, K. Z., Zhang, L., Wahl, L. M., and Suttles, J. (2005) TNF receptor-associated factor 6 is an essential mediator of CD40-activated proinflammatory pathways in monocytes and macrophages. *J. Immunol.* **174,** 1081–1090
31. Wong, B. R., Besser, D., Kim, N., Arron, J. R., Vologodskaia, M., Hanafusa, H., and Choi, Y. (1999) TRANCE, a TNF family member, activates Akt/PKB through a signaling complex involving TRAF6 and c-Src. *Mol. Cell* **4,** 1041–1049
32. Lomaga, M. A., Yeh, W. C., Sarosi, I., Duncan, G. S., Furlonger, C., Ho, A., Morony, S., Capparelli, C., Van G., Kaufman, S., van der Heiden, A., Itie, A., Wakeham, A., Khoo, W., Sasaki, T., Cao, Z., Penninger, J. M., Paige, C. J., Lacey, D. L., Dunstan, C. R., Boyle, W. J., Goeddel, D. V., and Mak, T. W. (1999) TRAF6 deficiency results in osteopetrosis and defective interleukin-1, CD40, and LPS signaling. *Genes Dev.* **13,** 1015–1024
33. Soriano, P., Montgomery, C., Geske, R., and Bradley, A. (1991) (1991) Targeted disruption of the c-Src proto-oncogene leads to osteopetrosis in mice. *Cell* **64,** 693–702
34. Arch, R. H., Gedrich, R. W., and Thompson, C. B. (1998) Tumor necrosis factor receptor-associated factors (TRAFs). A family of adapter proteins that regulates life and death. *Genes Dev.* **12,** 2821–2830
35. Ye, H., Arron, J. R., Lamothe, B., Cirilli, M., Kobayashi, T., Shevde, N. K., Segal, D., Dzivenu, O. K., Vologodskaia, M., Yim, M., Du, K., Singh, S., Pike, J. W., Darnay, B. G., Choi, Y., and Wu, H. (2002) Distinct molecular mechanism for initiating TRAF6 signaling. *Nature* **418,** 443–447
36. Chen, H., Wu, Y., Zhang, Y., Jin, L., Luo, L., Xue, B., Lu, C., Zhang, X., and Yin, Z. (2006) Hsp70 inhibits lipopolysaccharide-induced NF-kappaB activation by interacting with TRAF6 and inhibiting its ubiquitination. *FEBS Lett.* **580,** 3145–3152
37. Lamothe, B., Campos, A. D., Webster, W. K., Gopinathan, A., Hur, L., and Darnay, B. G. (2008) The RING domain and first zinc finger of TRAF6 coordinate signaling by interleukin-1, lipopolysaccharide, and RANKL. *J. Biol. Chem.* **283,** 24871–24880
38. Cates, E. A., Connor, E. E., Mosser, D. M., and Bannerman, D. D. (2009) Functional characterization of bovine TIRAP and MyD88 in mediating bacterial lipopolysaccharide-induced endothelial NF-κB activation and apoptosis. *Comp. Immunol. Microbiol. Infect. Dis.* **32,** 477–490
39. Yang, M., Omura, S., Bonifacino, J. S., and Weissman, A. M. (1998) Novel aspects of degradation of T cell receptor subunits from the endoplasmic reticulum (ER) in T cells. Importance of oligosaccharide processing, ubiquitination, and proteasome-dependent removal from ER membranes. *J. Exp. Med.* **187,** 835–846
40. Liu, A., Garg, P., Yang, S., Gong, P., Pallero, M. A., Annis, D. S., Liu, Y., Passaniti, A., Mann, D., Mosher, D. F., Murphy-Ullrich, J. E., and Goldblum, S. E. (2009) Epidermal growth factor-like repeats of thrombospondins activate phospholipase Cγ and increase epithelial cell migration through indirect epidermal growth factor receptor activation. *J. Biol. Chem.* **284,** 6389–6402
41. Sui, X. F., Kiser, T. D., Hyun, S. W., Angelini, D. J., Del Vecchio, R. L., Young, B. A., Hasday, J. D., Romer, L. H., Passaniti, A., Tonks, N. K., and Goldblum, S. E. (2005) Receptor protein-tyrosine phosphatase micro-regulates the paracellular pathway in human lung microvascular endothelia. (2005) *Am. J. Pathol.* **166,** 1247–1258
42. Toshchakov, V. U., Basu, S., Fenton, M. J., and Vogel, S. N. (2005) Differential involvement of BB loops of toll-IL-1 resistance (TIR) domain-containing adapter proteins in TLR4- *versus* TLR2-mediated signal transduction. *J. Immunol.* **175,** 494–500
43. Toshchakov, V. Y., Fenton, M. J., and Vogel, S. N. (2007) Cutting edge. Differential inhibition of TLR signaling pathways by cell-permeable peptides representing BB loops of TLRs. *J. Immunol.* **178,** 2655–2660
44. Yang, W. L., Wang, J., Chan, C. H., Lee, S. W., Campos, A. D., Lamothe, B., Hur, L., Grabiner, B. C., Lin, X., Darnay, B. G., and Lin, H. K. (2009) The E3 ligase TRAF6 regulates Akt ubiquitination and activation. *Science* **325,** 1134–1138
45. Tseng, P. H., Matsuzawa, A., Zhang, W., Mino, T., Vignali, D. A., and Karin, M. (2010) Different modes of ubiquitination of the adaptor TRAF3 selectively activate the expression of type I interferons and proinflammatory cytokines. *Nat. Immunol.* **11,** 70–75
46. Mansell, A., Brint, E., Gould, J. A., O'Neill, L. A., and Hertzog, P. J. (2004) Mal interacts with tumor necrosis factor receptor-associated factor (TRAF)-6 to mediate NF-κB activation by toll-like receptor (TLR)-2 and TLR4. *J. Biol. Chem.* **279,** 37227–37230
47. Verstak, B., Nagpal, K., Bottomley, S. P., Golenbock, D. T., Hertzog, P. J., and Mansell, A. (2009) MyD88 adapter-like (Mal)/TIRAP interaction with TRAF6 is critical for TLR2- and TLR4-mediated NF-kappaB proinflammatory responses. *J. Biol. Chem.* **284,** 24192–24203
48. Sasai, M., Tatematsu, M., Oshiumi, H., Funami, K., Matsumoto, M., Hatakeyama, S., and Seya, T. (2010) Direct binding of TRAF2 and TRAF6 to TICAM-1/TRIF adaptor participates in activation of the Toll-like receptor 3/4 pathway. *Mol. Immunol.* **47,** 1283–1291
49. Oda, H., Kumar, S., and Howley, P. M. (1999) Regulation of the Src family tyrosine kinase Blk through E6AP-mediated ubiquitination. (1999) *Proc. Natl. Acad. Sci. U.S.A.* **96,** 9557–9562
50. Harris, K. F., Shoji, I., Cooper, E. M., Kumar, S., Oda, H., and Howley, P. M. (1999) Ubiquitin-mediated degradation of active Src tyrosine kinase. *Proc. Natl. Acad. Sci. U.S.A.* **96,** 13738–13743
51. Rao, N., Miyake, S., Reddi, A. L., Douillard, P., Ghosh, A. K., Dodge, I. L., Zhou, P., Fernandes, N. D., and Band, H. (2002) Negative regulation of Lck by Cbl ubiquitin ligase. *Proc. Natl. Acad. Sci. U.S.A.* **99,** 3794–3799
52. Walsh, M. C., Kim, G. K., Maurizio, P. L., Molnar, E. E., and Choi, Y. (2008) TRAF6 autoubiquitination-independent activation of the NFκB and MAPK pathways in response to IL-1 and RANKL. *PLoS One* **3,** e4064
53. Wang, K. Z., Galson, D. L., and Auron, P. E. (2010) TRAF6 is autoinhibited by an intramolecular interaction which is counteracted by trans-ubiquitination. *J. Cell. Biochem.* **110,** 763–771
54. Pollet, I., Opina, C. J., Zimmerman, C., Leong, K. G., Wong, F., and Karsan, A. (2003) Bacterial lipopolysaccharide directly induces angiogenesis through TRAF6-mediated activation of NF-κB and c-Jun N-terminal kinase. *Blood* **102,** 1740–1742
55. Min, J. K., Cho, Y. L., Choi, J. H., Kim, Y., Kim, J. H., Yu, Y. S., Rho, J., Mochizuki, N., Kim, Y. M., Oh, G. T., and Kwon, Y. G. (2007) Receptor activator of nuclear factor (NF)-κB ligand (RANKL) increases vascular permeability: impaired permeability and angiogenesis in eNOS-deficient mice. *Blood* **109,** 1495–1502
56. Choi, Y. S., Choi, H. J., Min, J. K., Pyun, B. J., Maeng, Y. S., Park, H., Kim, J., Kim, Y. M, and Kwon, Y. G. (2009) Interleukin-33 induces angiogenesis and vascular permeability through ST2/TRAF6-mediated endothelial nitric oxide production. *Blood* **114,** 3117–3126
57. Zirlik, A., Bavendiek, U., Libby, P., MacFarlane, L., Gerdes, N., Jagielska, J., Ernst, S., Aikawa, M., Nakano, H., Tsitsikov, E., and Schönbeck, U. (2007) TRAF-1, -2, -3, -5, and -6 are induced in atherosclerotic plaques and differentially mediate proinflammatory functions of CD40L in endothelial cells. *Arterioscler. Thromb. Vasc. Biol.* **27,** 1101–1107
58. Carmeliet, P. (2000) Mechanisms of angiogenesis and arteriogenesis. *Nat. Med.* **6,** 389–395